9

The Continental Environment

In this chapter we will consider the geochemistry of lakes, rivers, and groundwater and processes that occur in the surface environment. It is this environment that is most susceptible to pollution. We will start by investigating the natural processes that determine the geochemistry of waters and soils. We will then investigate anthropogenic inputs and their effect on these systems and the modeling of the transport of metals and other species.

THE HYDROLOGIC CYCLE

The various reservoirs for surface water, and their water content, are listed in Table 9–1. The major reservoir for water, by a significant margin, is the oceans. The second major reservoir is the polar ice caps and glaciers. These two reservoirs account for 98.93% of the water at the earth's surface. Note that most of the rest of the surface water (1.09%) is contained in the groundwater reservoir. Thus, that portion of the water cycle that we are most familiar with (or aware of), the lakes and rivers, accounts for only a very small part of the total surface waters. However, this is the part of the hydrologic cycle that has the shortest residence times and is most susceptible to change. In Chapter 8 we discussed the atmospheric reservoir and in Chapter 10 we will consider the oceanic reservoir. In this chapter we will discuss rivers, groundwater, and lakes.

Table 9–1 *Inventory of Water at the Earth's Surface**

Reservoir	Volume 10^6 km^3	% of Total
Oceans	1400	95.96
Mixed layer	50	
Thermocline	460	
Abyssal	890	
Ice caps and glaciers	43.4	2.97
Groundwater	15.3	1.05
Lakes	0.125	0.009
Rivers	0.0017	0.0001
Soil moisture	0.065	0.0045
Atmosphere	0.0155	0.001
Terrestrial	0.0045	
Oceanic	0.0110	
Biosphere	0.002	0.0001
Total	1459	

*From Berner and Berner (1996).

The ***hydrologic cycle*** (Figure 9–1) *describes the transfer of water among the various water reservoirs.* Water evaporated from the ocean or rivers and lakes is transported through the atmosphere as water vapor. When this vapor condenses it reacts with gases and particulate matter in the atmosphere (see Chapter 8). These reactions lead to either acidic or basic precipitation, which contains various amounts of trace constituents. The precipitation may fall on either the ocean or the continents. Here we are concerned with the continental (land) portion of the cycle. If vegetation is present at the surface, the precipitation interacts with the vegetation and is modified by this interaction. This modification often consists of the addition of various organic molecules and interaction with dust particles attached to the vegetation. The precipitation subsequently flows to rivers and lakes by a series of processes including groundwater flow. A variety of rock (mineral)–water interactions occur during this transfer. These interactions, and their effect on water chemistry, are described in the following sections.

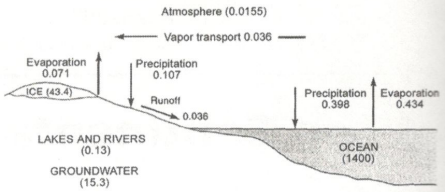

Figure 9–1
Schematic representation of the hydrologic cycle. Numbers in parentheses are the volume of water (10^6 km^3) in each reservoir. Fluxes are given in 10^6 km^3 y^{-1}. From Berner and Berner (1996).

WEATHERING

Weathering can be defined as *the various physical and chemical processes that lead to the decomposition of minerals and the breakdown of rocks to form soil.* This weathering is of two types: physical and chemical. Physical weathering (which is the mechanical breakdown of material) increases the surface-to-volume ratio so that subsequent chemical weathering, which is a surface process, is more effective. Chemical weathering takes place through interactions between water and gases and solid particles. For example, rainwater in equilibrium with atmospheric CO_2 has a pH of 5.7. In areas of acid input the rainwater can be even more acidic. These acid waters react with the minerals in rocks and soils, breaking down individual minerals and in the process releasing various species to the water, thus modifying its chemical composition. Chemical weathering is the major contributor of dissolved species to surface and ground waters.

There are four major types of chemical weathering: oxidation, congruent dissolution by water, congruent dissolution by acids, and incongruent dissolution by acids.

1. Oxidation occurs when oxygen reacts with minerals that contain reduced forms of various elements, usually Fe and S, and oxidizes these elements. As an example of this type of reaction, we can write the following equation for the oxidation of pyrite:

$$4FeS_{2\ \text{pyrite}} + 15O_2 + 8H_2O \rightarrow 2Fe_2O_{3\ \text{hematite}} + 8H_2SO_4$$

   Both Fe and S have been oxidized in this reaction. Hematite represents the final stable form that would be produced during this type of oxidation reaction, but intermediate species serve as precursors to the final product.

2. Congruent dissolution by water involves the simple dissolution of minerals, such as halite (NaCl) and anhydrite ($CaSO_4$), which are soluble in water. During congruent dissolution the ions go directly into solution, hence the dissolution of halite in water could be written

$$NaCl_{\ \text{halite}} \rightarrow Na^+ + Cl^-$$

3. Congruent dissolution by acids occurs when a mineral is dissolved by acid attack. In the natural environment this acid is often a soil acid formed by organic processes. However, for simplicity, we usually use carbonic acid when writing

equations for acid attack. The silicate minerals, olivine, pyroxene, and amphibole, and the carbonate minerals normally dissolve congruently. As examples, consider the dissolution of olivine by acid attack, which can be written

$$Mg_2SiO_{4\ \text{olivine}} + 4H_2CO_{3\ (aq)} \rightarrow 2Mg^2 + 4HCO_3^- + H_4SiO_{4\ (aq)}$$

and the dissolution of calcite by acid attack, which can be written

$$CaCO_{3\ \text{calcite}} + H_2CO_{3\ (aq)} \rightarrow Ca^{2+} + 2HCO_3^-$$

In these equations we have used the aqueous form of carbonic acid and the bicarbonate ion. As we know from previous discussions, the carbonate species actually present in solution depend on the pH. For the silicate weathering reaction, one of the products is aqueous silicic acid. Except at very high pH values, virtually all the silicic acid will exist in the nondissociated form.

4. Incongruent dissolution by acids occurs when a mineral breaks down to ions in solution and a solid of different composition. Most silicate minerals undergo incongruent dissolution. A typical reaction is the chemical decomposition of feldspar, which can be written

$$2NaAlSi_3O_{8\ \text{Na-plagioclase}} + 2H_2CO_{3\ (aq)} + 9H_2O \rightarrow Al_2Si_2O_5(OH)_{4\ \text{kaolinite}} + 2Na^+ + 2HCO_3^- + 4H_4SiO_{4\ (aq)}$$

The Na-plagioclase is converted to kaolinite with the concomitant release of Na^+ and Si to solution.

Table 9–2 lists the common rock-forming minerals and the usual chemical decomposition process(es). The *minerals that are decomposed by the chemical weathering process*

Table 9–2 Decomposition Reactions for Common Primary Minerals*

Mineral	Composition	Commonly occur in rock type(s)	Reaction
Olivine	$(Mg,Fe)SiO_4$	Igneous	Oxidation of Fe Congruent dissolution by acids
Pyroxenes	$(Mg,Fe)SiO_3$ $Ca(Mg,Fe)Si_2O_6$	Igneous	Oxidation of Fe Congruent dissolution by acids
Amphiboles	$Ca_2(Mg,Fe)_5Si_8O_{22}(OH)_2$ (also some Na and Al)	Igneous Metamorphic	Oxidation of Fe Congruent dissolution by acids
Plagioclase feldspar	$NaAlSi_3O_8$ to $CaAl_2Si_2O_8$	Igneous Metamorphic	Incongruent dissolution by acids
K-feldspar	$KAlSi_3O_8$	Igneous Metamorphic Sedimentary	Incongruent dissolution by acids
Biotite	$K(Mg,Fe)_3(AlSi_3O_{10})(OH)_2$	Metamorphic Igneous	Incongruent dissolution by acids Oxidation of Fe
Muscovite	$KAl_3Si_3O_{10}(OH)_2$	Metamorphic	Incongruent dissolution by acids
Volcanic glass (not a mineral)	Ca,Mg,Na,K,Al,Fe-silicate	Igneous	Incongruent dissolution by acids Incongruent dissolution by water
Quartz	SiO_2	Igneous Metamorphic Sedimentary	Resistant to dissolution
Calcite	$CaCO_3$	Sedimentary	Congruent dissolution by acids
Dolomite	$CaMg(CO_3)_2$	Sedimentary	Congruent dissolution by acids
Pyrite	FeS_2	Sedimentary	Oxidation of Fe and S
Gypsum	$CaSO_4 \cdot 2H_2O$	Sedimentary	Congruent dissolution by water
Anhydrite	$CaSO_4$	Sedimentary	Congruent dissolution by water
Halite	NaCl	Sedimentary	Congruent dissolution by water

*Adapted from Berner and Berner (1996).

are referred to as ***primary minerals***. The *minerals that are produced by the weathering process*, such as hematite, gibbsite, kaolinite, etc., are referred to as ***secondary minerals***.

In an old but classic study, Goldich (1938) investigated the breakdown of minerals in the weathering environment. Observational evidence suggested that there was a regular pattern to the order in which minerals in igneous and metamorphic rocks decomposed during chemical weathering. Other studies have essentially confirmed the original observations of Goldich. Based on these previous studies, Berner and Berner (1996) prepared a list of mineral weatherability (Table 9–3).

Table 9–3 Mineral Weatherability Listed in Order of Increasing Resistance to Weathering*

Halite
Gypsum, anhydrite
Pyrite
Calcite
Dolomite
Volcanic glass
Olivine
Ca-plagioclase
Pyroxenes
Ca-Na plagioclase
Amphiboles
Na-plagioclase
Biotite
K-feldspar
Muscovite
Vermiculite, smectite
Quartz
Kaolinite
Gibbsite, hematite, goethite

*Modified from Berner and Berner (1996).

The list is headed by the nonsilicate minerals halite, gypsum-anhydrite, pyrite, calcite, and dolomite. Halite is readily soluble in water. Gypsum and anhydrite are relatively insoluble in water, but calcite and dolomite are relatively soluble in acid waters. Thus, a thermodynamic explanation of the weatherability of these minerals is not straightforward. A free-energy calculation for the oxidation of pyrite yields a large negative free energy, indicating that the reaction should go spontaneously to the right; i.e., the oxidation of pyrite is thermodynamically favored.

The situation is different for the silicate minerals, and Curtis (1976) was able to show that the weatherability of silicate minerals did follow thermodynamic principles. The weathering reactions investigated by Curtis and their corresponding free energies are listed in Table 9–4. Also included in this table is the free energy for each reaction on a gram atom^{-1} basis. This last value is calculated by dividing the free energy of the reaction by the number of product atoms. This calculation is required because the free energy determined for the reaction is a function of the chemical equation used to describe the reaction, while we want to make our comparison on the basis of the number of product atoms. The order of weatherability determined by this approach is in good agreement with observational evidence. The order of weatherability determined from the thermodynamic calculations is olivine (fayalite and forsterite) → pyroxene (clinoenstatite and diopside) → amphibole (anthophyllite and tremolite) → anorthite (Ca-plagioclase) → albite (Na-plagioclase) → K-feldspar (microcline) → muscovite. With the exception of anorthite (Ca-plagioclase), this is the same order shown in Table 9–3, which was based on the observed breakdown of various silicate minerals in the weathering environment.

Table 9–4 Weathering Reactions and Free Energies per Gram Atom*

Mineral	Weathering reaction	ΔG_R^0 kJ mol^{-1}	ΔG_R^0 kJ (g atom)$^{-1}$
Fayalite	$Fe_2SiO_4 + \frac{1}{2}O_2 \rightarrow Fe_2O_3 + SiO_2$	−220.5	−27.53
Forsterite	$Mg_2SiO_4 + 4H^+ \rightarrow 2Mg^{2+} + 2H_2O + SiO_2$	−184.1	−16.74
Clinoenstatite	$MgSiO_3 + 2H^+ \rightarrow Mg^{2+} + H_2O + SiO_2$	−87.4	−12.47
Diopside	$CaMgSi_2O_6 + 4H^+ \rightarrow Mg^{2+} + Ca^{2+} + 2H_2O + 2SiO_2$	−159.4	−11.38
Anthophyllite	$Mg_7Si_8O_{22}(OH)_2 + 14H^+ \rightarrow 7Mg^{2+} + 8H_2O + 8SiO_2$	−574.0	−10.42
Tremolite	$Ca_2Mg_5Si_8O_{22}(OH)_2 + 14H^+ \rightarrow 5Mg^{2+} + 2Ca^{2+} + 8H_2O + 8SiO_2$	−515.5	−9.37
Anorthite	$CaAl_2Si_2O_8 + 2H^+ + H_2O \rightarrow Al_2Si_2O_5(OH)_4 + Ca^{2+}$	−100.0	−5.52
Albite	$2NaAlSi_3O_8 + 2H^+ + H_2O \rightarrow Al_2Si_2O_5(OH)_4 + 4SiO_2 + 2Na^+$	−96.7	−3.14
Microcline	$2KAlSi_3O_8 + 2H^+ + H_2O \rightarrow Al_2Si_2O_5(OH)_4 + 4SiO_2 + 2K^+$	−72.4	−1.34
Muscovite	$2KAl_3Si_3O_{10}(OH)_2 + 2H^+ + 3H_2O \rightarrow 2K^+ + 3Al_2Si_2O_5(OH)_4$	−72.4	−1.34

*Data from Curtis (1976).

Dissolution and Precipitation of Silica

After feldspar, the crystalline silica phases are the most abundant minerals in the rocks of the earth's crust. In most environments, quartz is very resistant to weathering. Amorphous silica occurs in deep-sea sediments and in volcanic rocks. Hence, an understanding of the behavior of silica compounds in the surface environment is necessary in order to describe the chemistry of surface waters. The dissolution of silica can be described by the following equation:

$$SiO_{2\,(s)} + 2H_2O \rightarrow H_4SiO_{4\,(aq)}$$

Rimstidt and Barnes (1980) developed the following equations for the solubility of silica compounds up to temperatures of about 200°C. For quartz,

$$\log K_{sp} = 1.8814 - 2.028 \times 10^{-3}T - \frac{1560.46}{T} \tag{9–1}$$

and for amorphous silica,

$$\log K_{sp} = 0.338037 - 7.8896 \times 10^{-4}T - \frac{840.075}{T} \tag{9–2}$$

where T is in Kelvin. Silicic acid ($H_4SiO_{4\,(aq)}$) is a weak acid, and its dissociation has been discussed in some detail in Chapter 3. At pH < 9.9, the dominant species is $H_4SiO_{4\,(aq)}$. At higher pHs, other species are dominant. The total silica in solution, as a function of pH, can be represented by the following equation (see Chapter 3):

$$Si_T = [H_4SiO_4]\left(1 + \frac{K_{a_1}}{[H^+]} + \frac{K_{a_1}K_{a_2}}{[H^+]^2}\right) \tag{9–3}$$

where K_{a_1} and K_{a_2} are the dissociation constants for the first and second dissociation steps. Solution of equations 9–1 and 9–2 for various temperatures gives us the concentration of $[H_4SiO_4]$ in solution. Equation 9–3 can then be used to determine the total silica in solution as a function of pH. At 25°C, solution of equations 9–1 and 9–2 gives $K_{sp} = 10^{-3.96}$ for quartz and $K_{sp} = 10^{-2.71}$ for amorphous silica. Assuming activity equals concentration, these solubility products are used to determine the total solubility of quartz and amorphous silica as a function of pH (Figure 9–2). Note that the solubility of both quartz and amorphous silica increases significantly at high pHs. This is because the dissociated forms of silicic acid become important contributors to the total amount of dissolved silica. In most natural environments, silica solubility will be low, but in environments such as alkaline lakes, relatively large amounts of silica will go into solution. Note that the behavior of silica is opposite to that of the carbonates, for which increasing pH leads to reduced

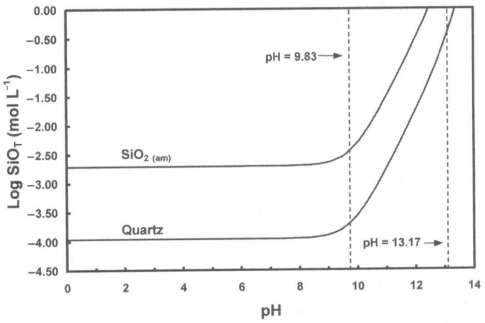

Figure 9–2
Solubility, at 25°C, of quartz and amorphous silica as a function of pH. pH = 9.83 and pH = 13.17 correspond to the first and second dissociation constants, respectively, of silicic acid.

solubility. These differences in behavior give rise to the common observation in the geologic record of silica replacing carbonates or vice versa, such replacements being controlled by the pH of the solutions.

Dissolution and Precipitation of Aluminum and Iron Hydroxides

The solubility of aluminum and iron hydroxides in the weathering environment exerts a significant influence on the transport of these elements in solution. In many weathering studies these two elements are considered to be immobile; i.e., they are believed to stay in the weathered material. Later in this chapter we will look at the effect of chelating agents on the transport of these, and other, species. Here we are concerned with the variation in solubility of the aluminum and iron hydroxides as a function of pH. The approach is similar to that already used for silica.

The dissolution of aluminum hydroxide can be written

$$Al(OH)_3 \rightarrow Al^{3+} + 3OH^-$$

For this reaction,

$$K_{sp} = [Al^{3+}][OH^-]^3 \tag{9–4}$$

Recall that $K_w = [H^+][OH^-]$. We can use this expression to substitute for OH^- in equation 9–4. After this substitution we have the following:

$$K_{sp} = [Al^{3+}]\left(\frac{K_w^3}{[H^+]^3}\right) = \frac{[Al^{3+}]K_w^3}{[H^+]^3} \tag{9–5}$$

Solving for Al^{3+} in solution,

$$[Al^{3+}] = \frac{K_{sp}[H^+]^3}{K_w^3} \tag{9–6}$$

The total solubility of aluminum in solution is the sum of the solubility of Al^{3+} plus all the Al-OH complexes.

$$\Sigma\ Al_{(aq)} = [Al^{3+}] + [AlOH^{2+}] + [Al(OH)_2^+] + [Al(OH)_{3\ (aq)}] + [Al(OH)_4^-] \tag{9–7}$$

For each of the complexes we can write a complexation reaction, and each of the complexation reactions has a corresponding equilibrium constant.

$$Al^{3+} + H_2O \rightleftharpoons AlOH^{2+} + H^+$$

and

$$K_{\beta_1} = \frac{[AlOH^{2+}][H^+]}{[Al^{3+}]} \tag{9–8}$$

$$Al^{3+} + 2H_2O \rightleftharpoons Al(OH)_2^+ + 2H^+$$

and

$$K_{\beta_2} = \frac{[Al(OH)_2^+][H^+]^2}{[Al^{3+}]} \tag{9–9}$$

$$Al^{3+} + 3H_2O \rightleftharpoons Al(OH)_{3\,(aq)} + 3H^+$$

and

$$K_{\beta_3} = \frac{[Al(OH)_{3\,(aq)}][H^+]^3}{[Al^{3+}]} \tag{9–10}$$

$$Al^{3+} + 4H_2O \rightleftharpoons Al(OH)_4^- + 4H^+$$

and

$$K_{\beta_4} = \frac{[Al(OH)_4^-][H^+]^4}{[Al^{3+}]} \tag{9–11}$$

Rearranging equations 9–8 through 9–11 and substituting into equation 9–7 gives

$$\Sigma\, Al_{(aq)} = [Al^{3+}] + \frac{K_{\beta_1}[Al^{3+}]}{[H^+]} + \frac{K_{\beta_2}[Al^{3+}]}{[H^+]^2} + \frac{K_{\beta_3}[Al^{3+}]}{[H^+]^3} + \frac{K_{\beta_4}[Al^{3+}]}{[H^+]^4} \tag{9–12}$$

Next we factor out $[Al^{3+}]$ and substitute equation 9–6 for $[Al^{3+}]$. The final equation is

$$\Sigma\, Al_{(aq)} = \frac{K_{sp}}{K_w^3}\left([H^+]^3 + K_{\beta_1}[H^+]^2 + K_{\beta_2}[H^+] + K_{\beta_3} + \frac{K_{\beta_4}}{[H^+]}\right) \tag{9–13}$$

The constants required to solve this equation are found in Table 9–5. The total aluminum in solution, as a function of pH, for a solution in equilibrium with gibbsite is shown in Figure 9–3 (p. 320). Note that the solubility is strongly pH dependent. The minimum solubility is found at pH ≈ 6.4, within the range of natural waters. Acidic and alkaline waters in equilibrium with gibbsite will contain large amounts of Al. This is a significant observation in terms of the aluminum content of acid streams and lakes and alkaline lakes. We will consider this topic further in a later section.

Ferric iron behaves similarly to Al^{3+}. The equation for total ferric iron in solution is identical to equation 9–13, except that the complexation and solubility constants are different (Table 9–5).

Table 9–5 Constants for Al and Fe^{3+} Solubility Calculations at 25°C*

Phase	pK_{sp}	pK_{β_1}	pK_{β_2}	pK_{β_3}	pK_{β_4}
$Al(OH)_{3\,(am)}$	31.2	5.00	10.1	16.9	22.7
$Al(OH)_{3\,gibbsite}$	33.9	5.00	10.1	16.9	22.7
$Fe(OH)_{3\,(am)}$	37.1	2.19	5.67	12.56	21.6
$Fe(OH)_{3\,goethite}$	44.2	2.19	5.67	12.56	21.6
	pK_0	pK_1	pK_2	pK_3	pK_4
Kaolinite	−3.72	1.28	6.38	13.18	18.98

*Data from Nordstrom et al. (1990) and Macalady et al. (1990).

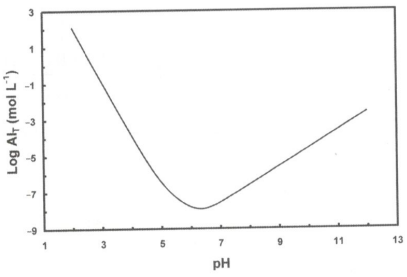

Figure 9–3
Total concentration of aluminum in solution, as a function of pH, for a solution in equilibrium with gibbsite.

In the next section, dealing with stability diagrams, we will find that at $[H_4SiO_{4\,(aq)}] \approx 10^{-4}$ mol L^{-1}, kaolinite replaces gibbsite $[Al(OH)_3]$ as the stable aluminum-containing phase. When this happens the aluminum solubility will be controlled by reactions involving kaolinite. Langmuir (1997) develops this equilibrium in detail. The resulting equation is given here and the appropriate constants are listed in Table 9–5.

$$\Sigma\, Al_{(aq)} = \frac{1}{[H_4SiO_{4\,(aq)}]}\left(K_0[H^+]^3 + K_1[H^+]^2 + K_2[H^+] + K_3 + \frac{K_4}{[H^+]}\right) \qquad (9\text{–}14)$$

Stability Diagrams

Stability diagrams are *graphical representations of equilibria between minerals and aqueous solutions*. Such diagrams are very useful in inferring what will happen when waters of various composition interact with solid phases. In this section we will go through the process of constructing one of these diagrams from thermodynamic data and then use the diagram to make inferences about what will happen during the weathering of silicate minerals. In order to simplify our calculations, we will assume that the solid phases are pure and fixed in composition and that aluminum is insoluble and remains in the solid phases. At low and high pH values, aluminum will enter solution, and the latter assumption will not be valid. As is always the case when making equilibrium thermodynamic calculations, the usefulness of these calculations in understanding natural processes is dependent on how close the reactions come to achieving equilibrium and the similarity between the solid phases used in the calculations and the solid phases in the natural environment.

From Table 9–2 we know that plagioclase and K-feldspar both break down by incongruent dissolution. Plagioclase and K-feldspar, along with quartz, are among the most abundant minerals in the earth's crust. We will construct a stability diagram that can be used to understand the chemical breakdown of Na-plagioclase to a variety of weathering products. We will also include on this diagram the stability limits for quartz and amorphous silica. The other stability diagrams of interest involve the chemical weathering of Ca-plagioclase and K-feldspar. The construction of these diagrams appears in the problem set. These stability diagrams were derived by Bricker and Garrels (1965) and Garrels (1984). In order to maintain consistency with the literature, Table 9–6 lists the thermodynamic values to be used in these calculations (including the problem set). All the calculations are done at 25°C.

We start by determining the equilibrium constants for the dissolution of quartz and amorphous silica. For quartz the reaction is

$$SiO_{2\,quartz} + 2H_2O \rightleftharpoons H_4SiO_{4\,(aq)}$$

This is an example of a hydrolysis reaction, another type of chemical weathering in which the solid reacts with H_2O. For this reaction, $\Delta G^0_R = 22.6$ kJ mol^{-1} and $K_{eq} = 10^{-3.96}$.

Table 9–6 *Thermodynamic Data for Stability Diagram Calculations*

Species or mineral	ΔG_R^0 kJ mol^{-1}	Source
Na^+	−261.9	Robie et al. (1978)
K^+	−282.5	Robie et al. (1978)
Ca^{2+}	−553.5	Robie et al. (1978)
H_2O	−237.15	Robie et al. (1978)
$H_4SiO_{4\ (aq)}$	−1308.0	Robie et al. (1978)
Quartz [SiO_2]	−856.3	Robie et al. (1978)
Amorphous SiO_2	−849.1	Drever (1997)
Albite [$NaAlSi_3O_8$]	−3711.7	Robie et al. (1978)
Microcline [$KAlSi_3O_8$]	−3742.3	Robie et al. (1978)
Anorthite [$CaAl_2Si_2O_8$]	−4017.3	Robie et al. (1978)
Muscovite [$KAl_3Si_3O_{10}(OH)_2$]	−5600.7	Robie et al. (1978)
Kaolinite [$Al_2Si_2O_5(OH)_4$]	−3799.4	Robie et al. (1978)
Pyrophyllite [$Al_2Si_4O_{10}(OH)_2$]	−5269.3	Garrels (1984)
Gibbsite [$Al(OH)_3$]	−1159.0	Garrels (1984)
Illite [$K_{0.8}Al_{1.9}(Al_{0.5}Si_{3.5})O_{10}(OH)_2$]	−5471.8	Garrels (1984)
Na-beidellite [$Na_{0.33}Al_{2.33}Si_{3.67}O_{10}(OH)_2$]	−5368.1	Langmuir (1997)
Ca-beidellite [$Ca_{0.167}Al_{2.33}Si_{3.67}O_{10}(OH)_2$]	−5371.6	Calculated
Montmorillonite [$K_{0.3}Al_{1.9}Si_4O_{10}(OH)_2$]	−5303.2	Garrels (1984)

Remember that for consistency we are using the data in Table 9–6, not equation 9–1 or 9–2. The equilibrium equation is

$$K_{eq} = 10^{-3.96} = [H_4SiO_{4\ (aq)}] \tag{9–15}$$

At equilibrium, $[H_4SiO_{4\ (aq)}] = 10^{-3.96}$ mol L^{-1}. A similar calculation for amorphous silica gives $\Delta G_R^0 = 15.4$ kJ mol^{-1}, $K_{eq} = 10^{-2.70}$, and at equilibrium $[H_4SiO_{4\ (aq)}] = 10^{-2.70}$ mol L^{-1}.

We can now write a set of equations that describe the interaction between solutions and various minerals during the incongruent dissolution of Na-plagioclase (albite). The phases (minerals) of interest are gibbsite, kaolinite, Na-beidellite (a montmorillonitic clay), and albite. For the reaction kaolinite → gibbsite,

$$Al_2Si_2O_5(OH)_{4\ \text{kaolinite}} + 5H_2O \rightleftarrows 2Al(OH)_{3\ \text{gibbsite}} + 2H_4SiO_{4\ (aq)}$$

For this reaction, $\Delta G_R^0 = 51.15$ kJ mol^{-1} and $K_{eq} = 10^{-8.96}$. The equilibrium equation is

$$K_{eq} = 10^{-8.96} = [H_4SiO_{4\ (aq)}]^2 \tag{9–16}$$

and at equilibrium $[H_4SiO_{4\ (aq)}] = 10^{-4.48}$ mol L^{-1}. For the reaction albite → gibbsite,

$$NaAlSi_3O_{8\ \text{albite}} + H^+ + 7H_2O \rightleftarrows Al(OH)_{3\ \text{gibbsite}} + 3H_4SiO_{4\ (aq)} + Na^+$$

For this reaction, $\Delta G_R^0 = 26.85$ kJ mol^{-1} and $K_{eq} = 10^{-4.70}$. The equilibrium equation is

$$K_{eq} = 10^{-4.70} = \frac{[Na^+][H_4SiO_{4\ (aq)}]^3}{[H^+]} \tag{9–17}$$

Note that there are three aqueous species, Na^+, H^+, and $H_4SiO_{4\ (aq)}$. Subsequent reactions will have the same three aqueous species. For the reaction albite → kaolinite,

$$2NaAlSi_3O_{8\ \text{albite}} + 2H^+ + 9H_2O \rightleftarrows Al_2Si_2O_5(OH)_{4\ \text{kaolinite}} + 4H_4SiO_{4\ (aq)} + 2Na^+$$

For this reaction, $\Delta G_R^0 = 2.55$ kJ mol^{-1} and $K_{eq} = 10^{-0.45}$. The equilibrium equation is

$$K_{eq} = 10^{-0.45} = \frac{[Na^+]^2[H_4SiO_{4\ (aq)}]^4}{[H^+]^2} \tag{9–18}$$

For the reaction Na-beidellite → kaolinite,

$$6Na_{0.33}Al_{2.33}Si_{3.67}O_{10}(OH)_{2\ \text{Na-beidellite}} + 2H^+ + 23H_2O \rightleftarrows 7Al_2Si_2O_5(OH)_{4\ \text{kaolinite}} + 8H_4SiO_{4\ (aq)} + 2Na^+$$

For this reaction, $\Delta G_R^0 = 79.45$ kJ mol^{-1} and $K_{eq} = 10^{-13.92}$. The equilibrium equation is

$$K_{eq} = 10^{-13.92} = \frac{[Na^+]^2[H_4SiO_{4\ (aq)}]^8}{[H^+]^2} \qquad (9\text{–}19)$$

For the reaction albite → Na-beidellite,

$$7NaAlSi_3O_{8\ \text{albite}} + 6H^+ + 20H_2O \rightleftarrows 3Na_{0.33}Al_{2.33}Si_{3.67}O_{10}(OH)_{2\ \text{Na-beidellite}} + 10H_4SiO_{4\ (aq)} + 6Na^+$$

For this reaction, $\Delta G_R^0 = -30.8$ kJ mol^{-1} and $K_{eq} = 10^{5.40}$. The equilibrium equation is

$$K_{eq} = 10^{5.40} = \frac{[Na^+]^6[H_4SiO_{4\ (aq)}]^{10}}{[H^+]^6} \qquad (9\text{–}20)$$

We have now written equations for all the reactions of interest in the weathering of albite. Given the aqueous species, on our diagram we will plot $\log([Na^+]/[H^+]$ versus $\log[H_4SiO_{4\ (aq)}]$. For the kaolinite → gibbsite reaction, the only aqueous species is $H_4SiO_{4\ (aq)}$. For the other reactions, all three aqueous species are present. The easiest way to plot these reactions is to select two Na^+/H^+ ratios and then calculate the corresponding activity of $H_4SiO_{4\ (aq)}$ from the equilibrium equations. The curves are plotted in Figure 9–4a. Inspection of the crossover points leads to delineation of the stability fields for each mineral. These stability fields are plotted in Figure 9–4b, along with the saturation curves for quartz and amorphous silica.

Stability diagrams can be used to understand chemical changes that occur during water–rock (mineral) interactions. With reference to Figure 9–4b, we will consider two cases—closed system and open system. The curve labeled A through F in Figure 9–4b shows the path that will be taken during the weathering of albite in a closed system. We start with albite in equilibrium with a solution of composition A. This is a situation that

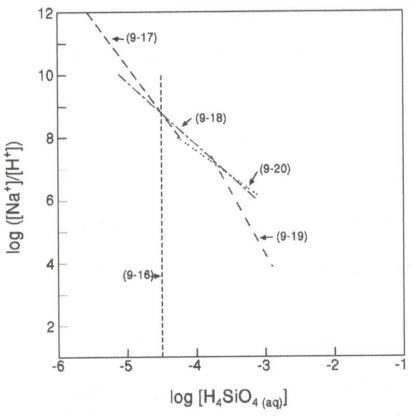

Figure 9–4a
Equilibrium equations 9–16 to 9–20 plotted on a $\log([Na^+]/[H^+])$ versus $\log[H_4SiO_{4\ (aq)}]$ diagram. Numbers on the diagram indicate corresponding equations in the text.

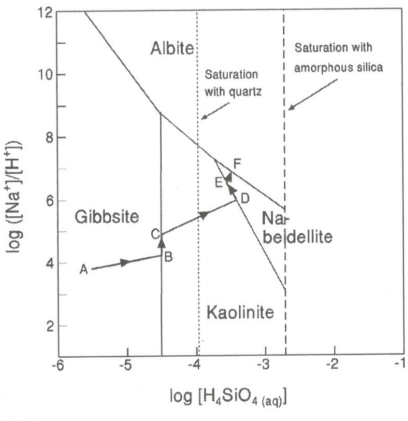

Figure 9–4b
Mineral stability fields as delineated by equilibrium equations plotted in Figure 9–4a. The labeled curve indicates the changes in chemistry of a solution in equilibrium with albite during weathering in a closed system. See text for discussion.

would exist during the start of weathering when a dilute solution is in contact with albite. We are in the gibbsite stability field and the weathering reaction can be written

$$NaAlSi_3O_{8\ albite} + H^+ + 7H_2O \rightarrow Al(OH)_{3\ gibbsite} + 3H_4SiO_{4\ (aq)} + Na^+$$

The conversion of albite to gibbsite involves the consumption of hydrogen ions and the release of silicic acid and sodium ions. Thus, both silicic acid activity and the sodium/hydrogen ratio of the solution increase and the solution follows the path A → B. When the gibbsite–kaolinite boundary is encountered, gibbsite is converted to kaolinite. The reaction can be written

$$2NaAlSi_3O_{8\ albite} + 4Al(OH)_{3\ gibbsite} + 2H^+ \rightarrow 3Al_2Si_2O_5(OH)_{4\ kaolinite} + 2Na^+ + H_2O$$

As long as gibbsite and kaolinite are present, the reaction will occur at constant silicic acid activity; i.e., the system is buffered in terms of silicic acid activity. This process is represented by segment B → C. After all the gibbsite is converted to kaolinite, the solution follows the path C → D and the reaction is

$$2NaAlSi_3O_{8\ albite} + 2H^+ + 9H_2O \rightarrow Al_2Si_2O_5(OH)_{4\ kaolinite} + 4H_4SiO_{4\ (aq)} + 2Na^+$$

During this reaction hydrogen ions are consumed and silicic acid and sodium ions are released to solution. The result is an increase in the Na^+/H^+ ratio and an increase in the activity of silicic acid. When the kaolinite–Na-beidellite boundary is encountered, kaolinite is converted to Na-beidellite. The reaction can be written

$$3NaAlSi_3O_{8\ albite} + 2Al_2Si_2O_5(OH)_{4\ kaolinite} + 2H^+ + 2H_2O \rightarrow$$
$$3Na_{0.33}Al_{2.33}Si_{3.67}O_{10}(OH)_{2\ Na\text{-}beidellite} + 2H_4SiO_{4\ (aq)} + 2Na^+$$

As long as kaolinite and Na-beidellite are present, the reaction will move along the boundary separating the stability field of these two minerals (D → E). After the kaolinite has been converted to Na-beidellite, the solution chemistry changes along the curve E → F until the Na-beidellite–albite stability boundary is reached.

For the open system, the important variable is the rate at which water moves through the weathering environment. This is sometimes referred to as the *flushing rate*. If we have high rainfall and good infiltration, the concentration of silicic acid and various ions in solution will be low. Under these conditions albite will weather to gibbsite. This is the situation observed in tropical settings where there is deep weathering and the weathered material largely consists of aluminum (gibbsite) and iron hydroxides. In regions of lower rainfall and less rapid infiltration, the concentration of ions in solution is greater and albite will weather to kaolinite or montmorillonitic clays. This is the situation usually observed in temperate settings. Hence, returning to our discussion of the formation of soils in Chapter 5, there is a relationship between soil type and climatic conditions (Case Study 9–1).

CASE STUDY 9–1
Variations in Clay Mineralogy as an Indicator of Paleoclimatic Conditions

Price et al. (2000) determined the oxygen isotope compositions for belemnite genera from the Speeton Clay Formation, Filey Bay, England. The Speeton Clay Formation, consisting of claystones and calcareous mudrocks, was deposited in an epicontinental sea during the Early Cretaceous, approximately 142 to 133 million years ago. The oxygen isotope data revealed that paleotemperatures had varied from approximately 9 to 15°C (see problem 56 in Chapter 6). The variations in paleotemperature were accompanied by variations in clay mineral content. Kaolinite was the dominant clay mineral when paleotemperatures were high, and smectite (e.g., Na-beidellite) was the dominant clay mineral when paleotemperatures were low. This variation in clay mineral content was related to climatic conditions in the continental source region, the high smectite content representing arid conditions and the high kaolinite content representing humid conditions. This inference is related to the idea of flushing rates discussed earlier. For an arid climate the flushing rate would be low and smectite would be the stable clay mineral (Figure 9–4b), whereas during humid conditions the flushing rate would be higher and kaolinite would be the stable clay mineral. Thus, the authors were able to use variations in clay mineral content to make inferences about climatic conditions in the Early Cretaceous.

Source: Price et al. (2000).

GEOCHEMISTRY OF SURFACE AND GROUND WATERS

We begin this section with a brief discussion of the convention used to distinguish between dissolved and suspended matter and the variability in water chemistry and the ways in which we can represent this variability. In standard water-chemistry analysis, water samples are first filtered to remove suspended particles. By convention, this filtration is done using a 0.45-μm filter. Anything that passes through this filter is considered to be in solution. Thus, the distinction between dissolved and suspended material is somewhat arbitrary. The important point, however, is that ***by convention substances less than 0.45 μm in size are considered to be in solution; i.e., they are dissolved species***. The significance of this criteria will be considered further later in the chapter.

Variations in River and Groundwater Chemistry

Chemical analysis of surface and ground waters reveals a wide variation in relative proportions and total concentrations of dissolved species (Table 9–7). Several methods are commonly used to graphically portray these variations in water chemistry and to classify water types.

Table 9–7 Compositions of Selected Surface and Ground Waters

	Concentration (mg L^{-1})									
	Ca^{2+}	Mg^{2+}	Na^{+}	K^{+}	Cl^{-}	SO_4^{2-}	HCO_3^{-}	SiO_2	TDS	Ref.
River										
Colorado	83	24	95	5.0	82	270	135	9.3	703	1
Columbia	19	5.1	6.2	1.6	3.5	17.1	76	10.5	139	1
Mississippi	39	10.7	17	2.8	19.3	50.3	117	7.6	265	1
Rio Grande	109	24	117	6.7	171	238	183	30	881	2
U. Rhine	41	7.2	1.4	1.2	1.1	36	114	3.7	307	3
U. Amazon	19	2.3	6.4	1.1	6.5	7.0	68	11.1	122	4
L. Amazon	5.2	1.0	1.5	0.8	1.1	1.7	20	7.2	38	4
L. Negro	0.2	0.1	0.4	0.3	0.3	0.2	0.7	4.1	6	4
Zambeze	9.7	2.2	4.0	1.2	1	3	25	12	58	1
Nile	25	7.0	17	4.0	7.7	9	134	21	225	1
Ganges	25.4	6.9	10.1	2.7	5	8.5	127	8.2	194	5
Yellow	42	17.7	55.6	2.9	46.9	71.7	182	5.1	424	6
Groundwater (dominant rock)										
Central Florida (carbonate)	34	5.6	3.2	0.5	4.5	2.4	124	12	—	7
Central Pennsylvania (carbonate)	83	17	8.5	6.3	17	27	279	—	—	8
Montana (sandstone)	3.0	7.4	857	2.4	71	1.6	2080	16	3098	9
New Mexico (gypsum)	636	43	17	—	24	1570	143	29	2480	9
California (serpentine)	34	242	184	18	265	6.6	1300	175	2226	9
Rhode Island (granite)	6.5	2.6	5.9	0.8	5	0.9	38	20	82	9
Maryland (gabbro)	5.1	2.3	6.2	3.2	1.0	9.2	37	39	109	9
Hawaii (basalt)	17	42	38	3.1	63	15	84	18	251	9
New Mexico (rhyolite)	6.5	1.1	38	2	17	15	77	103	222	10
North Carolina (mica schist)	17	1.7	6.4	1	1.1	6.9	69	29	98	10
West Virginia (sand and gravel)	58	13	23	2.8	39	116	101	10	338	10
Alabama (limestone)	46	4.2	1.5	0.8	3.5	4.0	146	8.4	222	10

References: [1]Meybeck (1979), [2]Livingstone (1963), [3]Zobrist and Stumm (1980), [4]Stallard (1980), [5]Sarin et al. (1989), [6]Gordeev and Siderov (1993), [7]Back and Hanshaw (1970), [8]Langmuir (1971), [9]Matthess (1982), [10]Hem (1970).

Graphical Representations of Water Chemistry Two types of diagrams are commonly used to portray water chemistry, Stiff and Piper. Stiff diagrams show the concentrations (in milliequivalents) of the major ions (both cations and anions) as a shape that gives both the relative abundance of the various species and the total abundance. Piper diagrams are trilinear representations of cation, anion, and combined cation and anion proportions. Piper diagrams are often used to classify water types. The following two examples illustrate the plotting of Stiff and Piper diagrams.

EXAMPLE 9–1 In this example we will plot the chemical data for the Columbia and Rio Grande rivers and the Pennsylvania groundwater (Table 9–7) on a Stiff diagram. The following table illustrates the calculation for the Columbia River water. We start by determining the concentration of each ion in millimoles per liter and then calculate the concentration of each ion in milliequivalents. The concentrations in milliequivalents are plotted on the Stiff diagram, as shown in Figure 9–5, and the various points are connected by straight lines. Note that the concentrations of the Na^+ and K^+ ions have been combined.

	Columbia River						
	Ca^{2+}	Mg^{2+}	Na^+	K^+	Cl^-	SO_4^{2-}	HCO_3^-
mg L^{-1}	19	5.1	6.2	1.6	3.5	17.1	76
mmol L^{-1}	0.47	0.21	0.27	0.04	0.1	0.18	1.25
meq L^{-1}	0.95	0.42	0.27	0.04	0.1	0.36	1.25

The shape of the field is a representation of the relative proportions of the various ions, and the size of the field represents the total ionic concentration. The Rio Grande river and Central Pennsylvania ground waters are also plotted in Figure 9–5. From the shape of the Stiff diagrams we can easily infer that the Rio Grande has a much greater concentration of all ionic species than the Columbia River and that the bicarbonate ion, relative to the sulfate ion, is much less important in the Rio Grande than it is in the Columbia River. Inspection of the Central Pennsylvania groundwater diagram reveals that the dominant cation is Ca^{2+} and the dominant anion is HCO_3^-, so this is a Ca-carbonate water. Stiff diagrams are particularly useful when plotted on a map because they give a graphical representation of regional variations in water chemistry.

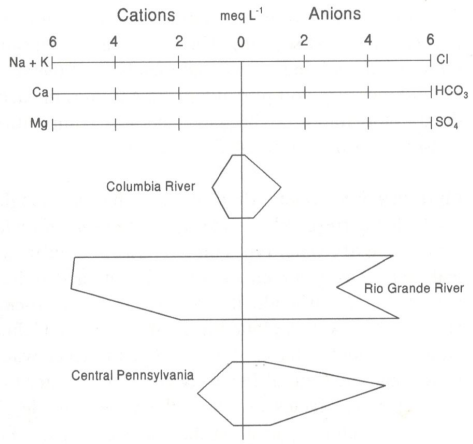

Figure 9–5
Stiff diagram for Columbia and Rio Grande river waters and Central Pennsylvania groundwater. See text for discussion. ■

EXAMPLE 9–2 In this example we plot the Columbia River data from Example 9–1 on a Piper diagram. As in Example 9–1, we start by calculating the concentration of each ion in milliequivalents. We now normalize the cations and the anions to 100% (as shown in the following table) so that we can plot them on the Piper diagram.

Cation concentrations			Anion concentrations		
	meq L^{-1}	Normalized		meq L^{-1}	Normalized
Ca^{2+}	0.95	56.5	Cl^-	0.10	5.8
Mg^{2+}	0.42	25.0	SO_4^{2-}	0.36	21.1
$Na^+ + K^+$	0.31	18.5	HCO_3^-	1.25	73.1
Total	1.68	100.0		1.71	100.0

The normalized cation and anion concentrations are plotted in their appropriate triangle (Figure 9–6). The data plotted on each triangle are then projected into the quadrilateral by drawing a line from the point on the cation triangle parallel to the Mg axis into the quadrilateral and by drawing a line from the point in the anion triangle parallel to the SO_4 axis into the quadrilateral. The intersection of these two lines marks the location of the point to be plotted on the quadrilateral (Figure 9–6). Symbols of different size are sometimes used to indicate differences in total dissolved species. This convention is used in the example. The data for the Rio Grande river and the Central Pennsylvania ground waters are also plotted in Figure 9–6. ■

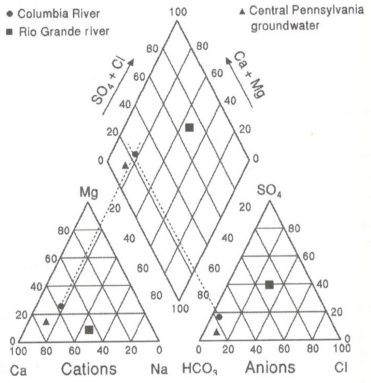

Figure 9–6
Piper diagram for Columbia and Rio Grande river waters and Central Pennsylvania groundwater. See text for discussion.

Piper diagrams have two main uses. The first is the graphical representation of water chemistry for the purpose of water classification (see the next section). The second is to determine if a series of water compositions represent the mixing of two end members. If the samples are the result of two-end-member mixing, they will plot along straight lines in each of the fields of the diagram. If they do not plot along straight lines, then their compositions are not controlled by simple two-end-member mixing (Case Study 9–2).

Hydrofacies Back (1966) divided the ion triangles of the Piper diagram into various fields that correspond to water type or *chemical facies* (Figure 9–7). This is a convenient way to classify water types on the basis of their major ion chemistry. Examples of chemical facies names are calcium bicarbonate and sodium chloride. If the water plots in the center of an ion triangle, it is referred to as *mixed-cation* or *mixed-anion facies*. With reference to the waters plotted in Figure 9–6, the Columbia River water belongs to the calcium-bicarbonate facies, the Rio Grande river water to the mixed-cation–mixed-anion facies, and the Central Pennsylvania groundwater to the calcium-bicarbonate facies. The hydrochemical facies in which the water sample plots potentially reveals information about the factors controlling the water chemistry. For example, the observation that the Columbia River water plots in the calcium-bicarbonate facies suggests that rock weathering is the major factor controlling water chemistry (see next section). The observation that the Central Pennsylvania groundwater plots in the calcium-bicarbonate facies suggests that dissolution of limestone, which would provide the Ca and bicarbonate ions, is important

CASE STUDY 9–2
Mixing of Acid Mine Drainage and Lake Water

In Case Study 2–1, Foos (1997) investigated the mixing of acid mine drainage from an abandoned coal mine with water discharged from a lake. The chemical compositions of the acid mine drainage, lake water, and the stream water downstream from the point of mixing were plotted on a Piper diagram (Figure 9–C2–1). This plot indicated that simple mixing would explain the concentrations of the major ions in the stream (mixed water). Further testing of the mixing model revealed that Ca^{2+}, Mg^{2+}, Na^{+}, K^{+}, and Cl^{-} concentrations could be explained by simple mixing, but not HCO_3^{-} and SO_4^{2-} concentrations. For HCO_3^{-} and SO_4^{2-}, the deviation from simple mixing was about 14%, so as a first approximation simple mixing is a reasonable assumption. The deviations from simple mixing for Fe^{2+} (1800%) and Mn^{2+} (39%) were significant. The reasons for the nonconservative behavior of these two species was discussed in Case Study 2–1. In this study, the Piper diagram was used to make an initial evaluation of the conservative versus nonconservative behavior of various species in solution.

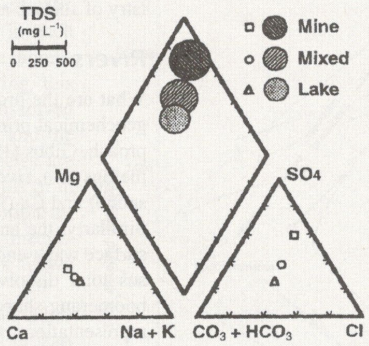

Figure 9–C2–1
Piper diagram showing the compositions of the mine and lake discharges and the mixed stream water. From Foos (1997).

Source: Foos (1997).

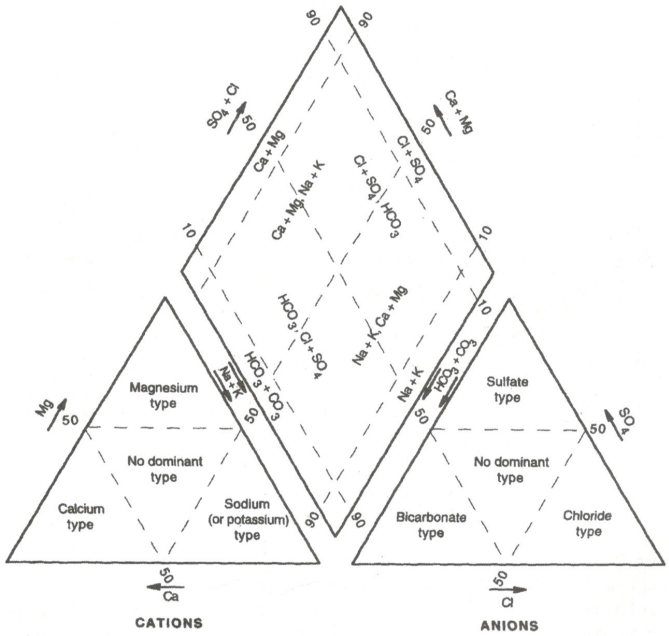

Figure 9–7
Hydrochemical facies. After Back (1966).

in determining the chemistry of the groundwater. The processes that determine the chemistry of surface and ground waters are considered further in the following sections.

Rivers

What are the processes that determine the chemical composition of rivers, and how can geochemical principles be used to answer this question? In a somewhat controversial approach, Gibbs (1970) investigated this question by summarizing the chemical data for numerous rain, river, lake, and ocean samples. In terms of cations, he considered Na (high saline) and Ca (freshwater) to be the best representatives of surface water end members. Similarly, the anions Cl (high saline) and HCO_3 (freshwater) were selected to represent surface water end members. Plots of the relative abundances of the cations and anions versus total dissolved solids (Figures 9–8a and 9–8b) gave two diagonal fields (and a boomerang-shaped diagram) anchored by the two end members. Based on these graphical representations, Gibbs suggested that there are three mechanisms that control the chemistry of surface waters. The first is atmospheric precipitation, which is represented by the surface waters with low total dissolved solids and relatively high Na and Cl that plot in the lower right portion of each diagram. The chemistry of most tropical rivers is presumably controlled by precipitation because these areas are well leached and there should be little contribution of dissolved materials from the rocks. The second mechanism is essentially weathering (referred to as *rock dominance*), in which the chemical breakdown of rocks (minerals) in the drainage basin provides the dissolved components. The positions in the

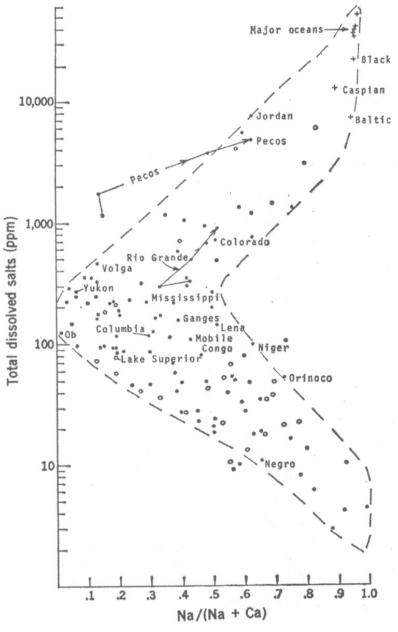

Figure 9–8a
Plot of total dissolved solids versus relative cation abundances for surface waters. Filled circles are river, unfilled circles are lake, and pluses are ocean waters. From "Mechanisms controlling world water chemistry by R. J. Gibbs in SCIENCE, 1970, #170, pp. 1088–1090. Copyright © 1970 American Association for the Advancement of Science. Reprinted with permission.

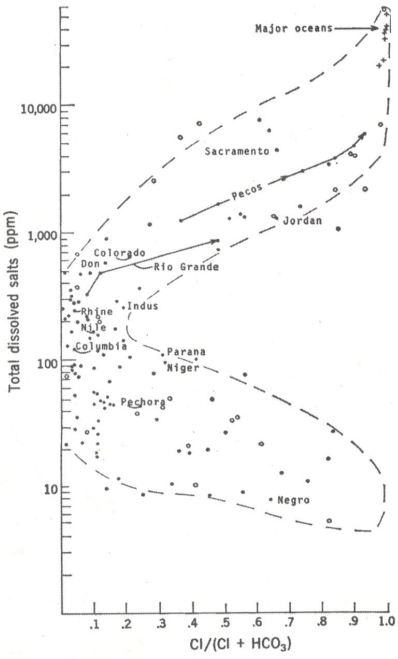

Figure 9–8b
Plot of total dissolved solids versus relative anion abundances for surface waters. Filled circles are river, unfilled circles are lake, and pluses are ocean waters. From "Mechanisms controlling world water chemistry by R. J. Gibbs in SCIENCE, 1970, #170, pp. 1088–1090. Copyright © 1970 American Association for the Advancement of Science. Reprinted with permission.

diagrams of waters that are controlled by this mechanism are determined by the climate, relief, and the rock types exposed in each basin. The third mechanism is evaporation–fractional crystallization. During this process the concentration of total dissolved solids increases due to evaporation and the concentrations of various ionic species are controlled by the precipitation of solids from solution as the total ionic concentration increases. The effect of these three mechanisms on surface water chemistry is shown graphically in Figure 9–9.

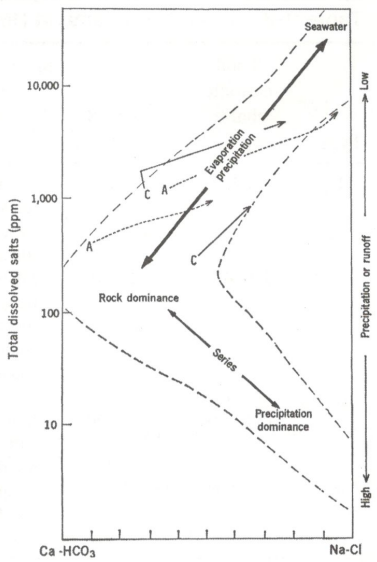

Figure 9–9
Graphical representation of the processes that control the chemistry of surface waters. See text for discussion. From "Mechanisms controlling world water chemistry" by R. J. Gibbs in SCIENCE, 1970, #170, pp. 1088–1090. Copyright © 1970 American Association for the Advancement of Science. Reprinted with permission.

A simple way to approach the Gibbs model of surface-water chemistry is to start with waters that are in partial equilibrium with the weathering products of their basin, the *rock dominance* field in Figure 9–9. We can envision two surface-water chemistry sequences. In the one, represented by the lower right part of the boomerang, the surface-water chemistry is a reflection of the relative importance of precipitation to groundwater + overland flow. If most of the ions are derived from precipitation, the chemistry of the surface waters will approximate that of dilute seawater. Remember from our discussion in Chapter 8 that one rainwater component can be viewed as dilute seawater. For the upper right arm of the boomerang, the controlling factor is the amount of evaporation and precipitation. For example, a river flowing through an arid landscape would be expected to show an increase in total dissolved solids as evaporation occurs and a decrease in Ca relative to Na due to the precipitation of calcium carbonate.

A number of authors have challenged the Gibbs model. The crux of the debate is the relative importance of weathering in determining the chemistry of rivers. This debate is particularly focused on the two ends of the boomerang. For example, for some rivers that plot in the lower right portion of the boomerang, it can be shown that the marine (i.e., precipitation) component is very small, leading to the conclusion that the ions are largely derived from weathering of rocks within the basin. For example, if carbonate and mafic igneous rocks are absent or of minor abundance, compared to rocks such as granite, one would expect Na to dominate over Ca. On the other hand, a number of the surface waters that plot in the upper right portion of the boomerang flow through regions that contain evaporite deposits, and it has been argued that it is the weathering of these deposits that is responsible for the high Na, Cl, and total dissolved solids content of these rivers. The Gibbs model also does not consider ion-exchange reactions that may occur between ions in solution and clay minerals. These reactions may be of significance in some cases. In summary, the objections to the Gibbs model are largely related to the significance of rock weathering, which many authors consider to be the most important process in determining the chemistry of surface waters. There are cases, however, where the Gibbs model provides a reasonable explanation for the surface-water chemistry.

Stallard and Edmond (1983) proposed a classification of river water chemistry that emphasizes the importance of rock weathering. Although this classification was developed specifically for the Amazon basin, it seems to have general applicability. The classification scheme is summarized in Table 9–8.

Table 9–8 Stallard and Edmond (1983) River Classification*

Type	Total cationic charge (μeq L^{-1})	~TDS (mg L^{-1})	Predominant source–rock type	Characteristic water chemistry (mole ratios)	Examples	Gibbs category
1	< 200	< 20	Intensely weathered (cation-poor) siliceous rocks and soils (thick regolith)	Si-enriched; low pH; Si/(Na + K) = 2; high Na/Na + Ca)	Amazon tributaries	Atmosphere-precipitation controlled
2	200–450	20–40	Siliceous (cation-rich); igneous rocks and shales (sedimentary silicates)	Si-enriched; (higher Si from igneous and metamorphic rocks); Si/(Na + K) = 2; intermediate Na/(Na + Ca) ~ 0.5	L. Amazon, Orinoco, Zaire	Between atmosphere-precipitation controlled and rock-dominated
3	450–3000	40–250	Marine sediments; carbonates, pyrite; minor evaporites	Na/Cl = l; (Ca +Mg)/(0.5HCO_3 + SO_4) = 1; low Na/(Na + Ca)	Most major rivers Rio Grande	Rock-weathering dominated
4	> 3000	> 250	Evaporites; $CaSO_4$ and NaCl	Na/Cl = 1; (Ca + Mg)/(0.5 HCO_3 + SO_4) = 1; high Na/(Na + Ca)		Evaporation–crystallization

*From Berner and Berner (1996).

The characteristic water chemistry of the various river types provides information about the material that is being weathered. For the first two river types, the rock that is weathered contains variable amounts of feldspar (K-feldspar and Na-plagioclase). We can write a weathering reaction for K-feldspar as follows:

$$2KAlSi_3O_{8\ \text{K-feldspar}} + 2H^+ + 9H_2O \rightarrow Al_2Si_2O_5(OH)_{4\ \text{kaolinite}} + 2K^+ + 4H_4SiO_{4\ (aq)}$$

Note that in this weathering reaction Si and K are released in a 2:1 ratio. A similar weathering reaction can be written for Na-plagioclase. For type 1 rivers, the Na/(Na + Ca) ratio is high because there is little Ca in the plagioclase and other Ca-bearing ferromagnesian silicates are rare. For type 2 rivers, there is a greater amount of Ca relative to Na due to an increase in the Ca content of the plagioclase in the rocks plus the presence of Ca-containing ferromagnesian silicates. For the type 3 rivers, Ca and Mg are significant because of the presence of carbonate-containing sediments. For the type 4 rivers, the high Na relative to Ca reflects the presence of evaporites. For the type 4 rivers, note that in basins that contain a significant amount of gypsum and/or anhydrite, the Ca content would be much more significant than the Na content. For the type 3 and type 4 rivers, representative evaporite and carbonate weathering reactions are

$$CaSO_4 \rightarrow Ca^{2+} + SO_4^{2-}$$

and

$$CaCO_3 + H_2CO_3 \rightarrow Ca^{2+} + 2HCO_3^-$$

For both reactions the $(Ca^{2+} + Mg^{2+})/(0.5HCO_3^- + SO_4^{2-})$ is 1:1. Hence, we would conclude that for the last two water types in Table 9–8 the weathering of carbonate rocks and evaporites is a major factor in determining their water chemistry.

Table 9–9 summarizes the relative importance of various sources for the ionic species found in river water. Note that contributions from pollution are included in the table and that for certain species pollution is a significant source. This is particularly notable for SO_4^{2-}, which has a predominant pollution source—mostly as acid deposition. Other sources of sulfate are natural biogenic emissions, volcanism, and the weathering of pyrite and other sulfide minerals.

Table 9–9 Sources of Major Elements in River Water (%)*

	Atmosphere	Weathering			
Species	Cyclic salt	Carbonates	Silicates	Evaporites	Pollution
Ca^{2+}	0.1	65	18	8	9
HCO_3^-	<< 1	61	37	0	2
Na^+	8	0	22	42	28
Cl^-	13	0	0	57	30
SO_4^{2-}	2	0	0	22	54
Mg^{2+}	2	36	54	<< 1	8
Na^+	1	0	87	5	7
H_4SiO_4	<< 1	0	> 99	0	0

*From Berner and Berner (1996).

In addition to the processes we have discussed, relief and climate also play a role in the chemistry of surface waters. Chemical weathering occurs at a maximum rate in wet and warm climates and at a minimum rate in dry and cold climates. The degree of relief determines the rapidity of the erosional process. For example, an area of low relief subjected to wet and warm climatic conditions would undergo extensive chemical weathering and most of the mobile components would be leached from the rocks and soil. This situation is typified by the type 1 river waters in Table 9–8. Streams draining the area have low total cation abundances. In an area of high relief, rapid erosion occurs and the time available for chemical weathering is reduced. Under these conditions we would expect chemical weathering processes, such as dissolution of evaporites, that proceed rapidly to contribute a substantially greater proportion of dissolved species to the streams than processes that occur much more slowly, such as the chemical breakdown of feldspar to kaolinite and dissolved species. For example, in an area of high relief where arkosic (feldspar-rich) sandstones are the major rock type, but minor amounts of evaporites or carbonate-bearing rocks exist, the latter rock types would disproportionately contribute to the dissolved load for the streams draining the area.

Groundwaters

A simplified groundwater system is shown in Figure 9–10. Precipitation infiltrates the subsurface materials and moves through the vadose zone to the zone of saturation. The boundary between the ***vadose zone*** (in which *the pores are not completely filled with water*) and the ***saturated zone*** (in which *the pores are completely filled with water*) is the water table. In the saturated zone the groundwater moves along curved flow paths to the point of discharge—in this case, a stream. The water entering the system (1) has essentially the same chemical composition as the precipitation. As the water moves through the vadose zone (2), its chemical composition changes due to additions of organic material and soluble salts. Below the water table (3), the water is isolated from the atmosphere and a variety of chemical changes can occur. As the water moves through the groundwater system, oxygen is consumed by the oxidation of dissolved organic carbon. This changes the oxidation–reduction potential of the system. A variety of rock (or sediment)–water interactions occur, which are controlled by the minerals present in the rocks (or sediments). If

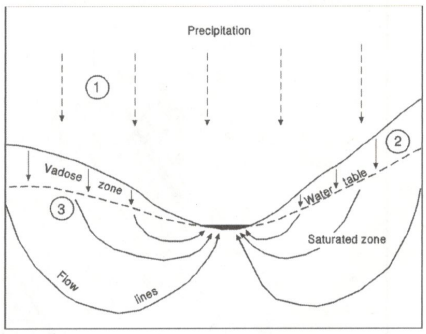

Figure 9–10
Simplified groundwater system showing the movement of water through the system. See text for discussion.

carbonates are present, their dissolution leads to changes in pH and P_{CO_2}. Soluble minerals, such as halite and gypsum, go into solution, adding various anions, such as Cl^- and SO_4^{2-}, to the groundwater. A number of important reactions occur between silicate minerals and the groundwater. These will be discussed more fully later. Because there is a kinetic factor involved in these reactions, the chemistry of the groundwater is modified as it moves through the groundwater system (Case Study 9–3).

Interactions between silicate minerals and groundwater are significant for aquifers consisting of sandstone, conglomerate, or fractured (or porous) igneous rock (and sediments of similar mineralogical composition). In what is now considered a classic paper, Garrels (1967) investigated the chemistry of groundwaters from igneous rocks and developed a model to explain it. The following assumptions are relevant to the construction of the model.

CASE STUDY 9–3
Chemical Evolution of Groundwater in the Floridian Aquifer System

We previously encountered the Floridian aquifer in Case Study 3–1. In that case study we were concerned with changes in pH, HCO_3^-, and P_{CO_2}. Here we will look at the variety of chemical changes that occur as groundwaters move through this aquifer. The Floridian aquifer occurs in a sequence of Tertiary carbonate rocks that underlie Florida and extend northward into Alabama, Georgia, and South Carolina. This is one of the most productive aquifers in the world and is a major source of drinking water for residents in the southeastern United States. One of the major recharge areas for the Floridian aquifer is in central Florida, and groundwater moves away from this recharge area (potentiometric high) toward the Gulf of Mexico and Atlantic Ocean. Along the coastal margins the groundwater mixes with seawater.

The chemical evolution of the waters in the Floridian aquifer, as they move away from the potentiometric high, is shown in Figure 9–C3–1. In the recharge area the waters are dominantly Ca^{2+} and HCO_3^-. As the water moves away from the recharge area, there are relative increases in the concentrations of Mg^{2+} and SO_4^{2-}. Finally, an increase in $Na^+ + K^+$ and Cl^- is observed in the discharge areas.

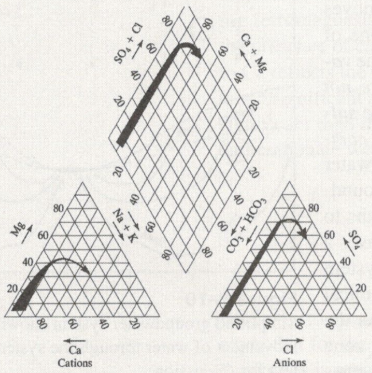

Figure 9–C3–1
Piper diagram showing chemical evolution of groundwater in the Floridian aquifer from recharge areas to discharge areas. From Back and Hanshaw (1970).

Why do these changes occur? In the recharge area the dominant process is calcite dissolution, which contributes the Ca^{2+} and HCO_3^- to the water. As the groundwater moves away from the recharge area, minor amounts of gypsum in the carbonate rock dissolve. The dissolution of gypsum releases Ca^{2+}, and the increase in Ca^{2+} concentration leads to oversaturation (due to the common ion effect) of the water in calcite. Dolomite [$CaMg(CO_3)_2$] is also present in the carbonate rocks, and as the calcite precipitates, dolomite dissolves. The combination of these three reactions—gypsum dissolution, calcite precipitation, and dolomite dissolution—leads to the observed increases in Mg^{2+} and SO_4^{2-}. Ion-exchange reactions also add Na^+ to the water. In the coastal discharge areas the groundwaters encounter modern or ancient seawater. Mixing with the seawater is responsible for the observed increases in Na^+ and Cl^- in the discharge areas.

The common ion effect was previously mentioned in Chapter 3 without explanation. Let us consider the dissolution of calcite. We can write the chemical reaction as follows:

$$CaCO_3 + H_2CO_3 \rightleftharpoons Ca^{2+} + 2HCO_3^-$$

For this reaction the equilibrium equation is

$$K_{eq} = [Ca^{2+}][HCO_3^-]^2$$

The dissolution of gypsum can be written

$$CaSO_4 \cdot 2H_2O \rightarrow Ca^{2+} + SO_4^{2-} + 2H_2O$$

During gypsum dissolution Ca^{2+} ions are released to solution (a common ion with respect to both gypsum and calcite solubility). The increase in Ca^{2+} ions in solution can lead to saturation of the solution in calcite and calcite precipitation. The other ion, SO_4^{2-}, released during gypsum dissolution does not participate in the calcite equilibrium reaction.

Source: Back and Hanshaw (1970).

1. Silicate minerals are decomposed through aggressive attack by waters that contain CO_2, i.e., acid attack by carbonic acid. Organic acids in soils can be a major contributor to the total acidity of soil waters, but treating all acid as carbonic is a reasonable simplification.
2. Plagioclase feldspars and the ferromagnesian silicate minerals (olivine, pyroxene, amphibole, and biotite) are attacked much more rapidly than K-feldspar or quartz.
3. K^+ and Mg^{2+} come chiefly from biotite and/or amphibole.
4. After correction for the rainwater Na^+, the Na^+ and Ca^{2+} in the groundwater are solely due to plagioclase dissolution. The correction for rainwater Na^+ is done by subtracting a molar amount of Na^+ from the analysis equal to the molar amount of Cl^-. An implicit assumption is that calcite, dolomite, or gypsum, all of which could contribute Ca^{2+} ions, are not present in the aquifer. Although it might be possible to correct for Ca^{2+} ions derived from the dissolution of gypsum, using the amount of SO_4^{2-}, this is an uncertain correction because the oxidation of sulfide minerals in the aquifer will also contribute SO_4^{2-}.

From the earlier section dealing with stability diagrams, we know that the common weathering products for plagioclase would be gibbsite, kaolinite, and smectites. Given the total ionic concentration of groundwaters, gibbsite is an unlikely phase. Hence, the two most important weathering products would be kaolinite and the smectite minerals (Garrels used montmorillonite, one of the smectites, in his model). Examples of weathering reactions for plagioclase feldspar to kaolinite are

$$8Na_{0.75}Ca_{0.25}Al_{1.25}Si_{2.75}O_{8\ \text{plagioclase}} + 10CO_2 + 15H_2O \rightarrow 5Al_2Si_2O_5(OH)_{4\ \text{kaolinite}} + 12SiO_{2\ (aq)} + 6Na^+ + 2Ca^{2+} + 10HCO_3^-$$

and

$$4Na_{0.5}Ca_{0.5}Al_{1.5}Si_{2.5}O_{8\ \text{plagioclase}} + 6CO_2 + 9H_2O \rightarrow 3Al_2Si_2O_5(OH)_{4\ \text{kaolinite}} + 4SiO_{2\ (aq)} + 2Na^+ + Ca^{2+} + 6HCO_3^-$$

The relative proportions of the soluble weathering products vary as a function of the composition of the plagioclase feldspar. For the first reaction, $Na^+/Ca^{2+} = 3$ and $HCO_3^-/SiO_{2\ (aq)} = 0.83$; for the second reaction, $Na^+/Ca^{2+} = 1$ and $HCO_3^-/SiO_{2\ (aq)} = 1.5$. By writing a number of these reactions, Garrels was able to construct the plagioclase–montmorillonite, plagioclase–kaolinite, and plagioclase–gibbsite curves shown in Figure 9–11.

The chemical compositions for waters from a number of igneous rocks tend to plot between the plagioclase–montmorillonite and plagioclase–kaolinite curves (Figure 9–11), suggesting that these waters are in equilibrium with mixed kaolinite–montmorillonite weathering products. Note that the agreement between theoretical and measured water compositions is best for volcanic (extrusive) rocks, with waters from rhyolites in equilibrium with oligoclase, waters from andesites in equilibrium with andesine, and waters from basalts in equilibrium with labroadorite, the appropriate plagioclase compositions for these rock types.

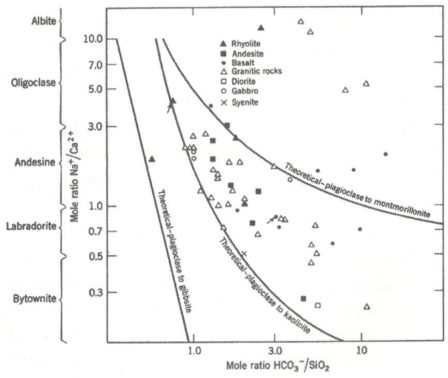

Figure 9–11
Mole ratio of Na^+/Ca^{2+} versus mole ratio of $HCO_3^-/SiO_{2\ (aq)}$ for waters from various types of igneous rocks. Most of the waters plot between the theoretical curves for the incongruent dissolution of plagioclase to montmorillonite and the incongruent dissolution of plagioclase to kaolinite. See text for discussion. From Garrels (1967).

The intrusive igneous rocks—granites, diorites, gabbros, and syenite—show a greater amount of scatter. One possibility is that the much larger grain size for the intrusive igneous rocks, and hence the much smaller surface-to-volume ratio, inhibits the approach to equilibrium. Although not a perfect match, the results of Garrels (1967) indicate that the chemical compositions of groundwaters are strongly affected by rock (mineral)–water interactions.

Garrels (1967) also investigated the question of whether or not the groundwaters were behaving as open or closed systems with respect to atmospheric CO_2. Figure 9–12 is a schematic diagram showing the approximate compositions of waters in equilibrium with some of the phases in the system CaO–Al_2O_3–SiO_2–H_2O. Calculated reaction paths for open and closed systems, starting with a plagioclase of composition $Na_{0.66}Ca_{0.34}Al_{1.34}Si_{2.66}O_8$, are shown in Figure 9–12. For the open system, $P_{CO_2} = 10^{-3.5}$ atm, and this pressure is maintained throughout the reaction. For the closed system, initial $P_{CO_2} = 10^{-1.5}$ atm (corresponding to dissolved $CO_2 = 0.001$ mol L^{-1}). As the reaction between H_2CO_3 and plagioclase proceeds, the composition of the waters changes, as shown by the arrows in Figure 9–12. Eventually, the boundary between the kaolinite and montmorillonite fields is reached, and at this point the waters are in equilibrium with both kaolinite and montmorillonite. The composition of the waters will then move along this stability boundary until all the kaolinite has been converted to montmorillonite. An important observation is that natural groundwaters tend to plot along the closed system curve and in the region above this curve. Virtually all the samples plot below the open system curve. This suggests that, in most cases, the chemical evolution of groundwater occurs in a closed system.

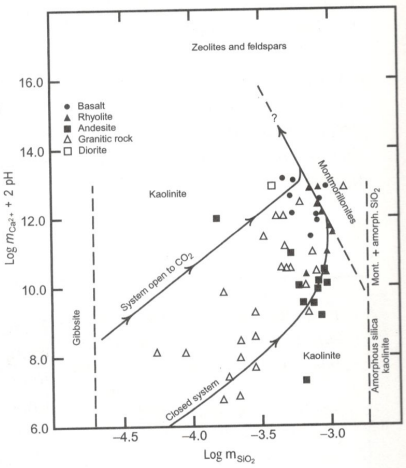

Figure 9–12
Plot of Ca^{2+} + pH versus SiO_2 for various groundwater samples. Stability boundaries for various phases are shown in the diagram. Solid curves with arrows indicate evolution of groundwater chemistry for systems open or closed with respect to atmospheric CO_2. See text for discussion. From Garrels (1967).

In summary, the preceding discussion suggests that there are several sources for the aqueous species found in groundwater. These are rainwater, dissolution of soluble minerals, and rock–water interactions. Table 9–10 lists the origin of the major aqueous species.

Lakes

Because of their complexity, in terms of physical, chemical, and biological processes, lakes have long attracted scientific interest. ***Limnology*** is *the study of lakes*. Lakes are of environmental interest because they can be readily affected by anthropogenic activities. For example, the addition of phosphorus to a lake by sewage effluent can lead to significantly enhanced primary biological production. Subsequent decay of the plant matter exhausts the oxygen from the lake waters, leading to anoxic conditions. This is an example of ***eutrophication***, which is *overnourishment of the lake*. As a second example, trace metals entering lakes can be removed by particles in the lake and sequestered in the bottom sediments, leading to a buildup of these trace metals.

Lakes can be viewed as temporary water storage reservoirs. Water input to lakes occurs by precipitation onto the lake surface, streams and rivers flowing into the lake, springs discharging into the lake, and groundwater flow into the lake. Water output occurs by evaporation, streams flowing out of the lake, and seepage through the lake floor. If the lake has been modified by anthropogenic activities, additional inputs and outputs can be via artificial channels. Most lakes have outlets, but in the case of interior drainage there may not

Table 9–10 *Origin of Major Aqueous Species in Groundwater**

Aqueous species	Origin
Na^+	NaCl dissolution (some pollution)
	Plagioclase weathering
	Rainwater addition
K^+	Biotite weathering
	K-feldspar weathering
Mg^{2+}	Amphibole and pyroxene weathering
	Biotite (and chlorite) weathering
	Dolomite weathering
	Olivine weathering
	Rainwater addition
Ca^{2+}	Calcite weathering
	Plagioclase weathering
	Dolomite weathering
HCO_3^-	Calcite and dolomite weathering
	Silicate weathering
SO_4^{2-}	Pyrite weathering (some pollution)
	$CaSO_4$ dissolution
	Rainwater addition
Cl^-	NaCl dissolution (some pollution)
	Rainwater addition
$H_4SiO_{4\,(aq)}$	Silicate weathering

*From Berner and Berner (1996).

be an outlet. In this case, water is lost via evaporation or seepage. This is a significant difference in that the concentration of dissolved species will increase in the lake waters, leading to high salt concentrations. Such lakes, sometimes referred to as *alkaline lakes*, are relatively common in arid areas.

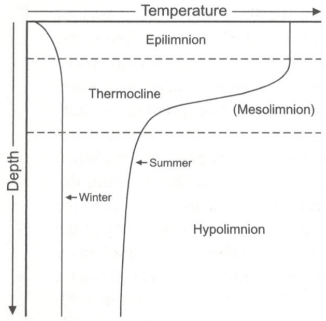

Figure 9–13
Generalized depth–temperature profiles for a midlatitude lake during the summer and winter.

Structure and Mixing of Lake Waters Mixing and overturn of lake waters are controlled by the water depth and climatic conditions. Mixing and overturn are important processes because they redistribute substances in the lake waters. For example, if overturn of water in the lake does not occur, or only occurs sporadically, deep waters may become enriched in some substances, such as organic matter, and depleted in other substances, such as dissolved oxygen. As a starting point for our discussion, we will look at the thermal structure of a midlatitude lake during the summer (Figure 9–13, summer curve). The lake is divided into three vertical layers: (1) the ***epilimnion***, which is the *well-mixed surface layer*; (2) the ***thermocline (or mesolimnion)***, which is a *zone of rapidly decreasing temperature*; and (3) the ***hypolimnion***, which is the *well-mixed deep layer*. With the onset of winter, the surface layer begins to cool and eventually reaches a temperature of 4°C, the temperature of maximum density for freshwater (Chapter 1). The denser surface waters now sink and the deeper, less dense waters are brought to the surface. As winter cooling continues, stratification returns to the lake with lower-density, colder waters overlying higher-density, warmer waters (winter curve in Figure 9–13). With the onset of summer the surface waters warm to 4°C and a second overturn will occur. Finally, the cycle is completed with a return to the summer temperature profile shown in Figure 9–13. In this case, two convective overturns have occurred. At lower latitudes (Mediterranean-type climates), winter temperatures do not reach 4°C. In this case, there is continuous mixing of water throughout the winter until stratification returns in the spring. At high latitudes, temperatures never get above 4°C. In this case, there is continuous mixing throughout the summer and then stratification during the winter when the lake is ice covered. In the tropics, air temperature is relatively constant throughout the year and there is no seasonally well-defined overturn. Other factors determine the overturn of the lakes under these

conditions. In certain unusual settings the absence of a seasonal overturn can lead to a natural disaster (Case Study 9–4). Shallow lakes are constantly stirred by wind action and a hypolimnion does not develop. Conversely, in the case of deep lakes a well-developed hypolimnion forms that is effectively isolated from the atmosphere.

Lake (Box) Models Substances can behave either conservatively or nonconservatively in any particular system. ***Conservative behavior*** occurs when the *variations in concentration of a substance can be described by simple mixing*. ***Nonconservative behavior*** occurs

CASE STUDY 9–4
"Killer Lakes" of the Cameroon Volcanic Line

The Cameroon volcanic line consists of a linear chain of Tertiary to Recent volcanoes extending from the Atlantic island of Pagalu to the interior of the African continent. Mount Cameroon is currently active, and there is ample evidence of recent volcanic activity throughout the continental portion of the province. Many of the volcanic craters are occupied by lakes. The Cameroon volcanic line occurs very close to the equator and the crater lakes do not have a seasonal overturn. On August 15, 1984, a lethal gas burst at Lake Monoun resulted in the death of 37 people. On August 21, 1986, a similar burst from Lake Nyos resulted in the death of more than 1700 people. Because of the loss of human life, and the unique character of the events, both lakes were subjected to intense scientific scrutiny.

Sigurdsson et al. (1987) reports the results of an extensive study of Lake Monoun, and the following description is derived from this paper. Lake Monoun is the result of a lava flow that formed a volcanic barrier lake. Subsequent volcanic activity formed two craters on the lake bottom. The larger crater in the eastern part of the lake extends to a depth of 96 m. Temperature measurements made in March of 1985 showed very little variation in surface temperatures (22.9 to 23.8°C) and deep-water temperatures of a similar value, around 22°C. The bottom sediments were predominantly fine-grained reddish brown silt composed of siderite, quartz, and kaolinite with minor muscovite, biotite, pyrite, and gibbsite. The siderite was considered to be an endogenic mineral (derived from within the lake), and the other minerals were considered to be allogenic (derived from outside the lake). Lake waters were anoxic below 50 m and the dominant species in solution were Fe^{2+} (~600 mg L^{-1}) and HCO_3^- ($\geq$ 1900 mg L^{-1}). When water samples were brought to the surface, large amounts of gas escaped from the samples. This gas was dominantly CO_2 with minor CH_4. Sulfur compounds were below detection in both the water and the gas. Oxygen and hydrogen isotopic analyses showed that the waters were stratified below about 15 m. The water in the hypolimnion plotted on the meteoric water line, indicating that magmatic waters are not present in the lake. Carbon isotopic data for both the dissolved bicarbonate and the CO_2 gas indicated a magmatic origin. Carbon isotopic data for methane suggested that this gas was produced by anaerobic bacterial reduction of organic matter. ^{14}C dating of the lake water revealed that only about 10% of the total carbon in the lake water was modern carbon. The authors concluded that the most likely scenario for the Lake Monoun disaster was the gradual buildup of CO_2 in the hypolimnion by degassing of a deeper magmatic source. Hydrothermal solutions were not involved, as indicated by the meteoric character of the water isotopic chemistry, the virtual absence of sulfur and chlorine (associated with hydrothermal activity), and the temperature of the lake water. Over a period of years, the release of CO_2 and the buildup of dissolved ferrous iron led to a siderite-saturated, higher-density hypolimnion within the larger lake bottom crater, overlain by a well-mixed, lower-density epilimnion. The lake was now density stratified and stable. This equilibrium was disturbed when a landslide occurred on the eastern rim of the crater lake, leading to the release of large volumes of CO_2 gas.

Lake Nyos occupies a 400-year-old (radiocarbon age) maar crater sited in Precambrian granite (Lockwood and Rubin, 1989). The lake is partly surrounded by poorly consolidated volcanic surge deposits. Field evidence suggests that carbon dioxide was the principal volatile involved in the formation of the maar. The maximum water depth is 220 m and, despite an increase in temperature with depth, the lake is density stratified due to the increase in dissolved species in the deeper waters. Like Lake Monoun, the deep waters are characterized by high concentrations of Fe^{2+} and HCO_3^-. Stable isotope ratios indicate a meteoric source for the lake water, but a mantle source for the carbon (Kusakabe et al., 1989). Kling et al. (1989) attributed an increase in bottom water alkalinity with time to the addition of thermal spring water. The mechanism responsible for the gas release is still uncertain. However, once deep water starts to ascend toward the surface, the process is self-sustaining. As the water rises, the hydrostatic pressure decreases and eventually equals the dissolved gas pressure. When this occurs, gas bubbles begin to form and the resulting decrease in density leads to a rapid rise of the deep waters to the surface. Of major concern is the integrity of the spillway at the northwest edge of the lake. At this location a 40-m-thick layer of pyroclastic material resting on granitic basement acts as a plug for the lake. The failure of this plug would result in a 40-m drop in water level and another catastrophic release of CO_2 from the deep waters. International efforts are now focused on decreasing the CO_2 concentration of the deeper waters so the lake level can be safely lowered. This degassing project involves the use of pipes that bring deep waters to the surface. The process is the same as described for the rise of the deep CO_2-rich waters, and, once initiated, the energy released during degassing is sufficient to drive the pumping operation.

Source: Sigurdsson et al. (1987), Lockwood and Rubin (1989), Kusakabe et al. (1989), Kling et al. (1989).

when *the concentration of a substance can be affected by processes other than simple mixing, i.e., by chemical and biological processes that occur within the system.* For example, a stream carrying iron in solution enters a lake. If the Eh and pH of the lake water is different from that of the stream, an iron–hydroxide flocculate may form and the iron is removed from solution. In this case, because it is removed, iron behaves as a nonconservative substance.

We can develop a generalized box model (Figure 9–14) for a lake that describes the behavior of both conservative and nonconservative substances (a similar model is applicable to the oceanic system). The lake is divided into two compartments, the epilimnion and hypolimnion. Additions to the epilimnion are by streams and transfer from the hypolimnion. Precipitation, airborne particles, and groundwater inputs are ignored. There may be cases where such inputs are significant and cannot be ignored in the calculation. For example, in Case Study 9–4, Sigurdsson et al. (1987) concluded that soil dust was the major source of the iron in Lake Monoun and Kling et al. (1989) concluded that thermal spring waters entering Lake Nyos were an important source of alkaline species. A substance is removed from the epilimnion by outflow, transfer to the hypolimnion, and as particles. In the case of chemical species, they may be removed as primary precipitates, by incorporation into the hard or soft parts of organisms, and by adsorption onto pre-existing particles. The removal of a species by particles can occur in the epilimnion and/or hypolimnion. Once formed, particles settle deeper into the lake, where changing chemical conditions may lead to re-solution of a species. For example, changes in Eh and pH may lead to the release of Fe and other Eh-sensitive elements to solution. For the epilimnion, we can write the following equation, which describes the change in amount of a substance with time:

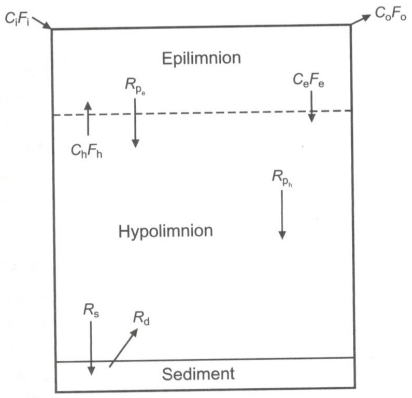

Figure 9–14
Two-compartment box model for a lake. See text for details.

$$\frac{\Delta M_e}{t} = C_iF_i + C_hF_h - C_oF_o - C_eF_e - R_{p_e} \qquad (9\text{–}21)$$

where ΔM_e is the change, with time, in the amount of the substance in the epilimnion, t is time, C_i is the concentration of the substance in the inlet water, F_i is the flux of water into the lake, C_h is the concentration of the substance in the hypolimnion, F_h is the flux of water from the hypolimnion to the epilimnion, C_o is the concentration of the substance in the outlet water, F_o is the flux of water out of the lake, C_e is the concentration of the substance in the epilimnion, F_e is the flux of water from the epilimnion to the hypolimnion, and R_{p_e} is the rate of removal of the substance by particles in the epilimnion. If the system is in a steady state, then $\Delta M_e/t = 0$ and equation 9–21 becomes

$$C_iF_i + C_hF_h = C_oF_o + C_eF_e + R_{p_e} \qquad (9\text{–}22)$$

For the hypolimnion, we can write the following equation for the change in the amount of a substance with time:

$$\frac{\Delta M_h}{t} = C_eF_e + R_d - C_hF_h - R_{p_h} \qquad (9\text{–}23)$$

where ΔM_h is the change, with time, in the amount of the substance in the hypolimnion, R_d is the rate of re-solution of the substance, and R_{p_h} is the rate of removal of the substance by particles in the hypolimnion. If the system is in a steady state, equation 9–23 becomes

$$C_eF_e + R_d = C_hF_h + R_{p_h} \qquad (9\text{–}24)$$

The amount of the substance that is ultimately stored in the sediment is

$$R_s = R_{p_e} + R_{p_h} - R_d \tag{9–25}$$

where R_s is the rate at which the substance is sequestered in the sediment.

Conceptually, it is important to understand the significance of each term in equation 9–25. In most cases, a certain amount of recycling will occur in the epilimnion. For example, phosphorus is a nutrient element and will be incorporated in organic matter. Some of this organic matter will break down in the epilimnion and the phosphorus will be returned to the water column. Therefore, R_{p_e} represents the net amount of the substance (in this case, phosphorus) removed from the epilimnion by particles. Similarly, R_{p_h} represents the net amount of a substance removed by particles from the hypolimnion. R_d is the amount of the substance returned to solution by interaction between the bottom waters and the sediments plus the release of the substance from particles originating in the epilimnion.

EXAMPLE 9–3 The concentration of Fe^{2+} in the epilimnion remains constant. Stream water inflow is 100 $m^3\ s^{-1}$ and the stream waters have an Fe^{2+} concentration of 3 mg L^{-1}. The lake is located in a temperate region and there is a net addition of water by precipitation (precipitation − evaporation) of 20 $m^3\ s^{-1}$. In order for the lake to maintain a constant volume, the outflow must be 120 $m^3\ s^{-1}$. The outflow has a mean Fe^{2+} concentration of 1.5 mg L^{-1}. Calculate the rate at which Fe^{2+} is removed from the epilimnion by particles. Assume that the Fe^{2+} concentration is the same for the epilimnion and the hypolimnion so the transfer of Fe^{2+} between the two layers can be ignored. Remember that 1 m^3 = 1000 L.

Rearranging equation 9–22 and solving gives

$$\begin{aligned} R_{p_e} &= C_iF_i - C_oF_o = (3000\text{ mg m}^{-3})(100\text{ m}^3\text{ s}^{-1}) - (1500\text{ mg m}^{-3})(120\text{ m}^3\text{ s}^{-1}) \\ &= 120{,}000\text{ mg s}^{-1} = 120\text{ g s}^{-1} \end{aligned}$$

Suppose that Fe^{2+} was not homogeneously distributed and that the concentration of Fe^{2+} was 2 mg L^{-1} in the epilimnion and 3 mg L^{-1} in the hypolimnion. If the volume of the epilimnion and hypolimnion remains constant, $F_e = F_h$. If $F_e = F_h = 500\ m^3\ s^{-1}$, calculate the rate at which Fe^{2+} is removed from the epilimnion as particles.

Rearranging equation 9–22 and solving gives

$$\begin{aligned} R_{p_e} &= C_iF_i + C_hF_h - C_oF_o - C_eF_e \\ R_{p_e} &= (3000\text{ mg m}^{-3})(100\text{ m}^3\text{ s}^{-1}) + (3000\text{ mg m}^{-3)}(500\text{ m}^3\text{ s}^{-1}) \\ &\quad - (1500\text{ mg m}^{-3})(120\text{ m}^3\text{ s}^{-1}) - (2000\text{ mg m}^{-3})(500\text{ m}^3\text{ s}^{-1}) \\ &= 620{,}000\text{ mg s}^{-1} = 620\text{ g s}^{-1} \end{aligned}$$

■

For a lake in a steady state, the total input of a substance to the lake must equal its total output. With reference to Figure 9–14, we see that there is only one input, rivers and streams flowing into the lake (but don't forget that there are other possible inputs such as precipitation and soil dust), and two outputs, water flowing out of the lake plus accumulation of the substance in the sediments. In this case, we can represent the rate of accumulation of the substance in the sediments as

$$R_s = C_iF_i - C_oF_o \tag{9–26}$$

For a system that is in a steady state, we can calculate both a residence time and a relative residence time for any substance. *The length of time, on average, that a substance remains in a lake* is referred to as the ***residence time***. As you will recall from Chapter 1, if a system is in a steady state (inputs = outputs) with respect to a particular substance, the residence time can be calculated from the following relationship:

$$\text{Residence time} = \frac{\text{Total amount of substance}}{\text{Rate of input (output)}} \tag{9–27}$$

We can also calculate the ***relative residence time***, which is the *residence time of a particular substance compared to the residence time of water*. If the lake volume remains constant, water acts as a conservative constituent. Comparison of other substances to water

allows us to differentiate conservative from nonconservative behaviors. If a substance has a relative residence time of 1, then it shows conservative behavior. Values other than 1 indicate nonconservative behavior. If the relative residence time is greater than 1, the substance accumulates in the lake. If the relative residence time is less than 1, the element is removed from the lake water to the sediment. We can derive a very simple relationship for relative residence time.

$$\tau_{rel} = \frac{\tau_s}{\tau_w} = \frac{M/C_i F_i}{V/F_i} = \frac{C_l V/C_i F_i}{V/F_i} = \frac{C_l}{C_i} \tag{9–28}$$

where τ_s is the residence time for the substance, τ_w is the residence time for the water, V is the volume of water in the lake, C_l is the concentration of the substance in the lake water, and M is the total mass of the substance in the lake ($M = C_l V$).

EXAMPLE 9–4 A lake has achieved steady-state conditions with respect to Fe, Cl, and P. For the incoming water, Fe = 4 mg L^{-1}, Cl = 14 mg L^{-1}, and P = 6 μg L^{-1}. For the lake water, Fe = 3.5 mg L^{-1}, Cl = 14 mg L^{-1}, and P = 10 μg L^{-1}. Calculate the relative residence time for each substance.

For Fe,

$$\tau_{rel} = \frac{C_l}{C_i} = \frac{3.5 \text{ mg L}^{-1}}{4.0 \text{ mg L}^{-1}} = 0.88$$

For Cl,

$$\tau_{rel} = \frac{C_l}{C_i} = \frac{14 \text{ mg L}^{-1}}{14 \text{ mg L}^{-1}} = 1.0$$

For P,

$$\tau_{rel} = \frac{C_l}{C_i} = \frac{10 \text{ } \mu\text{g L}^{-1}}{6 \text{ } \mu\text{g L}^{-1}} = 1.67$$

The calculations indicate that Cl acts as a conservative species, Fe acts as a nonconservative species (removed by sequestration in the lake sediments), and P acts as a nonconservative species (added because of recycling by biological processes). ■

pH of Surface and Ground Waters

In Chapter 3 we explored acid–base equilibria in some detail. Here we will look at specific processes that affect the pH of surface and ground waters and consider the impact of acid deposition on pH, an environmentally important topic. Recall from Chapter 3 that the carbonate system exerts the major control on the pH of natural waters. On a longer time frame, water–rock interactions can also exert a significant control on pH. We will consider both of these systems, plus other factors, in the following discussion.

There are three processes that determine the pH of surface and ground waters:

1. Ion-exchange reactions that occur between silicate minerals (particularly clay minerals in the soil horizon) and acid waters in which H^+ ions in solution are adsorbed by the clay minerals. We will discuss ion exchange in a subsequent section.
2. Buffering reactions involving the carbonic acid system. In this case, the important parameter is the availability of bicarbonate (HCO_3^-).
3. Water–rock interactions involving carbonate and silicate minerals.

Carbonic Acid System We discussed this buffer system at some length in Chapter 3. Figure 9–15 (p. 340) shows the distribution of the various species as a function of pH. The calculations have been done for a total carbonate content of 1×10^{-3} mol L^{-1}, a typical value for surface waters, and a temperature of 25°C. Except in very alkaline waters, the buffering reaction is

$$H^+ + HCO_3^- \rightleftharpoons H_2CO_{3\,(aq)}$$

The effectiveness of this buffer is determined by the availability of HCO_3^-, which is determined by the pH of the system. When $H^+ = HCO_3^-$, there is no longer any buffering capacity. For the case shown here, this equality occurs at pH = 4.65. For waters with lower amounts of total carbonate, the buffering capacity is lost at even higher pH values (see problem 87). Consider the impact of acid rain or acid mine runoff on this system. If the pH of the acid rain or acid mine runoff is less that 4.65, continued addition of these acid waters will lower the pH of the system until all buffering capacity is lost. As the pH decreases, the buffering capacity decreases (see Chapter 3, Figure 3–7) and, thus, the rate of pH decline increases; i.e., the acidification of surface waters is an accelerating process.

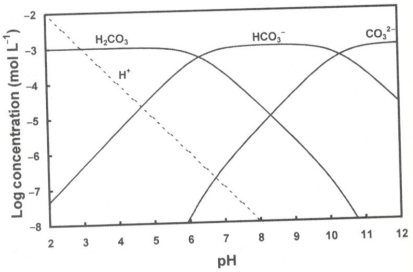

Figure 9–15
Variations in the concentration of the various carbonate species as a function of pH, in freshwater at a temperature of 25°C, given a total carbonate concentration of 1×10^{-3} mol L^{-1}. For these conditions the carbonate system loses its buffering capacity at pH = 4.65.

Water–Mineral Interactions Waters in contact with carbonate minerals will tend to have basic pH values. In Chapter 3 we determined that water saturated with calcite and in equilibrium with atmospheric CO_2 would have a pH of 8.26. We also determined the buffering capacity as a function of pH for this system (Figure 3–8). Waters in equilibrium with carbonate minerals have a significant capacity to resist pH changes. Groundwaters in equilibrium with carbonate minerals will also have basic pH values. If we add acid to the calcite-carbonate system, the following reaction occurs:

$$H^+ + CaCO_{3\ \text{calcite}} \rightarrow Ca^{2+} + HCO_3^-$$

This reaction replenishes bicarbonate ion that has been consumed in the buffering reaction. It also releases Ca^{2+} (and if dolomite is involved, Mg^{2+}) to the water. This is one reason why lakes that have been subjected to acid inputs tend to have higher concentrations of Ca and Mg than nonacidic lakes.

The other important set of pH-controlling reactions involves the silicate minerals. We considered several of these reactions in Chapter 3. Other silicate mineral–water reactions that may be important in consuming hydrogen ions are

$$Al_2Si_2O_5(OH)_{4\ \text{kaolinite}} + 6H^+ \rightarrow 2Al^{3+} + 2H_4SiO_{4\ (aq)} + H_2O$$
$$NaAlSi_3O_{8\ \text{albite}} + 4H_2O + 4H^+ \rightarrow Na^+ + Al^{3+} + 3H_4SiO_{4\ (aq)}$$

and

$$KMg_{1.5}Fe_{1.5}(AlSi_3O_{10})(OH_2)_{\text{biotite}} + 10H^+ \rightarrow K^+ + 1.5Mg^{2+} + 1.5Fe^{2+} + Al^{3+} + 3H_4SiO_{4\ (aq)}$$

Note that these reactions release Al^{3+} and other ions. One characteristic of acid lakes is an increase in dissolved aluminum, which is often correlated with a decline in fish populations. Recall from our discussion earlier in the chapter of aluminum solubility that decreasing pH leads to a greater solubility for aluminum. The other cations released to solution can be used to fingerprint the hydrogen-consuming mineral reactions. For example, the albite reaction leads to an increase in Na^+ and the biotite reaction releases K^+, Mg^{2+}, and Fe^{2+}. There is a stoichiometric relationship between these various ionic species, and in the case of our biotite example, the ratio of the ions should be K^+: $1.5Mg^{2+}$: $1.5Fe^{2+}$. In regions where mafic and ultramafic igneous rocks (in which olivine and pyroxene are common minerals) are abundant, the following silicate mineral–water reactions can lead to strongly alkaline waters:

$$Mg_2SiO_{4\ \text{forsterite}} + 4H^+ \rightarrow 2Mg^{2+} + H_4SiO_{4\ (aq)}$$

and

$$MgSiO_{3\ \text{enstatite}} + 2H^+ + 2H_2O \rightarrow Mg^{2+} + H_4SiO_{4\ (aq)}$$

These waters also tend to have high concentrations of bicarbonate ion and, thus, high buffering capacities.

ADSORPTION–DESORPTION PROCESSES

The adsorption (and desorption) of inorganic and organic species by particles plays an important role in the distribution of these species in the environment. As discussed in Chapter 7, the smaller the size of a particle, the greater the surface-to-volume ratio. The surface area of the particle is a critical factor in adsorption–desorption processes because broken bonds are found at the surface and this is where the particle has a net electrostatic charge exposed to the surrounding solution. This surface charge arises because of (1) substitutions of cations of lesser charge for cations of higher charge in the crystal structure or (2) reactions involving functional groups on the mineral surface and ions in solution. The charge due to ion substitution is considered to be fixed, whereas the charge due to surface complexation is variable and depends on the pH of the solution. The binding of the charged species to the surface is a function of several factors, including the charge density at the surface, the total charge, and the competing charged species in solution. If we look at this process in terms of the solution, there are several important factors: (1) pH, (2) oxidation–reduction potential, and (3) ionic strength of the solution. What this means is that changing environmental conditions influence whether or not a particular species is adsorbed or released by particles.

For particles that have a fixed charge (i.e., the 2:1 clay minerals), the net negative charge is balanced in several ways. (1) *Cations may attach directly to oxygen ions (or more precisely, silanol functional groups, Chapter 7) exposed at the particle surface.* This type of complex is called an ***inner-sphere complex*** and the bonds are relatively strong. (2) *Cations that are surrounded by water molecules (sometimes called solvated cations) are attached to the particle surface by bonds between the water molecules and exposed surface functional groups.* This type of complex is called an ***outer-sphere complex***. These are much weaker bonds and outer-sphere complex ions are readily exchanged with ions in solution. (3) The remainder of the negative charge is balanced by a diffuse layer of ***counter ions***, *cations that surround the mineral surface.* These cations are not attached to the mineral surface. In the so-called *diffuse double layer*, the positive counter ions are more abundant than the negative co-ions, which offsets the remaining negative surface charge.

For particles that do not have a fixed charge (e.g., 1:1 clays, oxyhydroxides), the surface charge is variable and varies as a function of pH. In this case, the charge is due to complexation reactions involving surface hydroxyls. At low pH values, the surface hydroxyls combine with H^+ in solution to form positively charged surface complexes:

$$S\text{–}OH + H^+ \rightarrow S\text{–}OH_2^+$$

where S represents a surface metal cation (Al^{3+}, Mg^{2+}, Fe^{3+}, etc.). The end result of this reaction is a positively charged surface. With increasing pH the hydrogen ions will return to solution, as represented by the following reaction:

$$S\text{–}OH + OH^- \rightarrow S\text{–}O^- + H_2O$$

The result of this reaction is a negatively charged surface. There are also other possible types of surface complexation reactions that involve metal cations and negatively charged ligands.

In summary, the surface charge of a particle is a function of a number of different processes. We can write the following equation to represent these relationships:

$$NC = FC + NP + ISC + OSC \qquad (9\text{–}29)$$

where NC is the net charge, FC is the fixed charge due to substitutions in the crystal structure,

Table 9–11 Point of Zero Net Proton Charge*

Material	pH_{pznpc}	Material	pH_{pznpc}
α-$Al(OH)_3$	5.0	δ-MnO_2	2.8
γ-AlOOH	8.2	SiO_2	2.0
Fe_3O_4	6.5	Feldspars	2–2.4
α-FeOOH	7.8	Kaolinite	4.6
α-Fe_2O_3	8.5	Montmorillonite	2.5
$Fe(OH)_{3\ (am)}$	8.5	Albite	2.0

*From Kehew (2001).

NP is the net proton charge due to the binding or release of hydrogen ions from the surface, ISC is the charge due to the presence of inner-sphere complexes, and OSC is the charge due to the presence of outer-sphere complexes. If the net charge is not zero, it is balanced by the ions in the diffuse double layer adjacent to the surface. In equation 9–29, with the exception of the fixed charge, all the charge components on the right-hand side vary as a function of pH. Because charge varies as a function of pH, the surface may be either negatively or positively charged. It follows that there is some *pH at which the surface has no charge* ***(point of zero charge, PZC)***. We can also define a ***point of zero net proton charge***, ***PZNPC*** (Table 9–11), which occurs *when the charge due to the binding and release of protons (NP) is zero* (see Chapter 7 for further details). At pH values below these points of zero charge, the particle has a positively charged surface; at pH values above the zero point charge, the particle has a negatively charged surface. Hence, the relationship between pH and surface charge is an important factor in determining the adsorptive characteristics of particles.

Adsorption of Metal Cations

The adsorption of metal cations varies as a function of their ionic potential. ***Ionic potential*** is the *ratio of the charge of the cation divided by its radius*—in effect, the charge density of the surface of the cation. Ions that have low ionic potential more readily lose their attached water molecules and, hence, form inner-sphere complexes. As noted, inner-sphere complexes are more tightly bound to the surface of the particle. For ions of the same charge, the selectivity series (order in which the ions are preferentially adsorbed, from most strongly adsorbed to least strongly adsorbed) is simply related to ionic radius. Increasing ionic radius leads to lower ionic potential. For example, consider the first column of elements in the periodic table, all of which form +1 ions. With reference to Appendix III, the ionic radii for these ions (in VI-fold coordination) are Li (0.82), Na (1.10), K (1.46), Rb (1.57), and Cs (1.78). The selectivity series for this group of ions is

$$Cs^+ > Rb^+ > K^+ > Na^+ > Li^+$$

For the elements in the second column, the order would be

$$Ba^{2+} > Sr^{2+} > Ca^{2+} > Mg^{2+}$$

For metals in the transition series, the electron configuration becomes more important than ionic radius in determining selectivity. For example, the following selectivity series has been established for a subset of the transition metals:

$$Cu^{2+} > Ni^{2+} > Co^{2+} > Fe^{2+} > Mn^{2+}$$

As noted, when the adsorbing particles have variable surface charge, pH becomes an important factor. At low pH, the surface is positively charged, and at higher pH, above the PZNPC, the surface becomes negatively charged. Once the surface becomes negatively charged, metals are rapidly adsorbed by the surface over a relatively narrow pH range (Figure 9–16). The degree of adsorption increases with increasing pH because the nega-

tive surface charge is increasing. Within any particular group of charged ions, those with higher selectivity are adsorbed at lower pH values. Of particular importance here is to note that changing pH exerts a significant influence on the adsorption of various metal cations. Hence, changes in pH can lead to either adsorption of cations from solution or desorption of cations from particles.

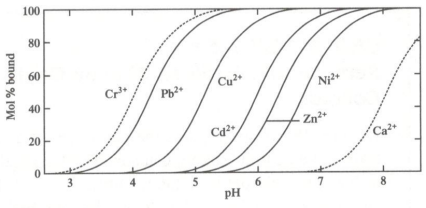

Figure 9–16
Adsorption of metal cations as a function of pH. From AQUATIC CHEMISTRY, 3rd Edition by W. Stumm and J. J. Morgan. Copyright © 1996. This material is used by permission of John Wiley & Sons, Inc.

Colloids

The types of particles involved in adsorption–desorption reactions can be mineral particles (Chapter 7), organic particles (Chapter 5), and colloids. As mentioned previously, by definition a species is in solution if it passes through a 0.45-μm filter. Molecular-size species pass through this filter, as expected, but a portion of the colloidal size range is less than 0.45 μm and colloids will also pass through the filter. ***Colloids*** are *particles that occupy the size range between true solutions and suspensions. This size range is not precisely defined but is generally considered to encompass particles between 10 μm and 0.01 μm in diameter. In this size range Brownian motion plays an important role in maintaining particle suspension.* In natural waters colloids are usually clay minerals, silica, oxyhydroxides, organic matter, and bacteria. The colloidal size range and amount vary as a function of the hydrologic environment (Table 9–12).

Colloidal sizes vary as a function of the dynamics of the hydrologic environment. Rapidly moving water carries much larger colloidal particles than slow-moving water. For example, most groundwater, which has a very low velocity, only transports very small colloidal particles. But note the much larger colloidal particles found in the Noiraigue spring, which is located in a karst topography where high groundwater flow velocities would be expected. In general, the greatest absolute amounts of colloidal particles are found in rivers, largely because of the high input of dissolved materials. Even in the case of systems with low absolute and relative amounts of colloidal particles, colloidal particles can be major transporters of metals because of their small size and correspondingly large surface area. This is particularly true when the colloidal particles are clay minerals, which have large specific surface areas (Chapter 7).

Table 9–12 Size Ranges for Colloidal Particles in Natural Waters*

Sample	Amount (mg L^{-1})	Size observed (μm)	Size peaks (μm)
Rainwater	0.006	0.08	
Northern Pacific Ocean		0.38–1	
Gulf of Mexico		0.02–8	
Biscayne Bay		0.5–150	
Lake		0.04–0.4	0.1
Chuckawa Creek	50	0.3–1.3	0.2
Mississippi River	350		0.3
Yarra River	1–10	0.1–0.5	0.22
Noiraigue spring	0.5–10	0.5–60	0.8–1
Groundwater (Gorleben)			0.005–0.01
Groundwater (Grimsel)	0.1	0.04–1	

*Data from Atteia et al. (1998).